Transverse spin relaxation in inhomogeneous magnetic fields

S. D. Stoller and W. Happer
Department of Physics, Princeton University, Princeton, New Jersey 08544

F. J. Dyson
Institute for Advanced Studies, Princeton, New Jersey 08540
(Received 25 April 1991)

We discuss the transition between two limiting cases of transverse spin relaxation due to magnetic-field inhomogeneities: very fast spatial diffusion, when the spins relax exponentially with time, and very slow spatial diffusion, when the spins relax exponentially with the cube of the time. Both limiting cases as well as intermediate cases can be described in terms of Airy functions, which are the eigenfunctions of the time-independent Torrey equation. Branch points in the eigenvalue spectrum and other interesting properties follow from the fact that the Torrey equation is not self-adjoint.

PACS number(s): 76.60.Es; 31.15.+q; 87.71.Kb

I. INTRODUCTION

If a sample of nuclear spins, initially in thermal equilibrium, is rotated by 90° away from the direction of the mean magnetic field with a short $\pi/2$ pulse, the spins subsequently twist about the mean magnetic field into a spiral-staircase pattern, since the spins in regions of stronger magnetic field process faster than spins in regions of weaker field. If the spins are fixed in space, there is no increase in entropy, and Hahn [1] showed that the initial polarization can be fully recovered by applying a π pulse, which leads to the formation of a spin echo. However, if the molecules can diffuse through the sample, as is the case for liquids or gases, not all of the spin polarization can be recovered in an echo experiment. The fraction of polarization remaining if an echo is formed at a time t after the $\pi/2$ pulse is [1–3]

$$\exp\frac{-D|\nabla\Omega_z|^2t^3}{3}, \tag{1.1}$$

where D is the diffusion coefficient of the spin-bearing molecules or atoms in the liquid or gas, and Ω_z is the component of the local Larmor frequency along the z axis. Physically, the irreversible decay described by (1.1) occurs because molecules diffuse from regions where the spins have rotated more into regions where the spins have rotated less.

According to (1.1), damping due to diffusion should increase indefinitely as D gets larger. However, the constraints of the container walls, which are not considered in (1.1), become crucial when a spin can diffuse from the interior to the cell wall during the decay time of the polarization. Recent studies of the effects of magnetic-field inhomogeneities have shown that at low gas pressures, the transverse spin polarization does not "twist" significantly, but remains nearly uniform within the sample volume due to the rapid diffusion. For a spherical cell of radius R, the magnitude of the spin polarization in this *motional narrowing* regime decays as [4]

$$\exp\frac{-8|\nabla\Omega_z|^2R^4t}{175D}. \tag{1.2}$$

Formulas analogous to (1.2) for cylindrical cells are given by McGregor [5]. The form of (1.2) is slightly different for very rapid diffusion [4]. The predictions of (1.1) and (1.2) are in excellent agreement with experimental results for slow or fast diffusion, and can be used to deduce quite accurate values of diffusion coefficients from measurements in either regime. The main qualitative differences between the two regimes are as follows:

(1) In the slow-diffusion regime (1.1), the magnitude of the spin polarization damps exponentially with the cube of the time. In the fast-diffusion regime (1.2), the damping is exponential with the first power of the time.

(2) Decreasing the diffusion coefficient D leads to slower damping in the slow-diffusion regime but to faster damping in the fast-diffusion regime.

(3) The damping rate is proportional to the fourth power of the cell diameter in the fast-diffusion regime but independent of the cell dimensions in the slow-diffusion regime.

In this paper we show how the transition occurs between these two regimes.

As in Refs. [4, 6, 7], we describe the atoms with a density matrix $|\rho)$ which is a function of the spatial position $\mathbf{r}$ of spins within the sample. The rate of change of the spin density matrix is given by Eq. (18) of Hasson *et al.* [7],

$$\frac{\partial}{\partial t}|\rho) = (-i\boldsymbol{\Omega}\cdot\mathbf{S} + D\nabla^2)|\rho). \tag{1.3}$$

Here $\mathbf{S}$ is the spin operator for $|\rho)$, that is, the infinitesimal rotation operator for the polarization of the spins. Equation (1.3) describes simultaneous spin rotation at the local Larmor frequency $\boldsymbol{\Omega}$ and spatial diffusion through the gas with the diffusion coefficient D. We ignore any other relaxation mechanisms in (1.3). We also assume no spin relaxation at the walls. Then at any point

on the wall, $|\rho)$ must obey the boundary condition

$$\mathbf{n}\cdot\nabla|\rho) = 0, \tag{1.4}$$

where the unit vector $\mathbf{n}$ is normal to the cell surface. Some of the interesting phenomena which are produced by walls which cause partial depolarization of the spins are described by Wu *et al.* [8], who use the more general boundary condition $\mathbf{n}\cdot\nabla|\rho) = -\mu|\rho)$, where μ is the normal gradient operator.

We will write the local Larmor frequency as

$$\Omega(\mathbf{r}) = \hat{\mathbf{z}}\Omega + \mathbf{r}\cdot\nabla\Omega, \tag{1.5}$$

the sum of a spatially homogeneous mean Larmor frequency of magnitude Ω, which defines the z axis of a coordinate system, and an inhomogeneous correction $\mathbf{r}\cdot\nabla\Omega$, which is linear in the displacement $\mathbf{r}$ from the center of the cell. We assume that $\nabla\Omega$ is a spatially constant tensor.

As described in Ref. [7], we expand the density matrix $|\rho)$ onto Fano's [9] irreducible basis tensors $|SM)$, which describe the spin polarization of the gas. For gas atoms with a nuclear spin quantum number K, we can have $S = 0, 1, \ldots, 2K$ for the angular momentum quantum number S of the tensor. The coefficients $(SM|\rho)$ of the basis tensors are functions of the position $\mathbf{r}$ and of the time t. For magnetic resonance experiments the amplitudes

$$(1\mu|\rho) = \left(\frac{3}{K(K+1)(2K+1)}\right)^{1/2}\langle K_\mu\rangle \tag{1.6}$$

are of particular interest, where the position-dependent expectation values of the nuclear spin in spherical and Cartesian basis systems are related by $\langle K_0\rangle = \langle K_z\rangle$ and $\mp\sqrt{2}\langle K_{\pm1}\rangle = \langle K_x\rangle \pm i\langle K_y\rangle$.

Projecting out the $|11)$ component of (1.3) we find

$$\frac{\partial}{\partial t}(11|\rho) = (-i\Omega + D\nabla^2)(11|\rho) - i\mathbf{r}\cdot\nabla\Omega_z(11|\rho) - \frac{i}{\sqrt{2}}\mathbf{r}\cdot\nabla(\Omega_x - i\Omega_y)(10|\rho). \tag{1.7}$$

If $\nabla\Omega = 0$, that is, if the magnetic field is perfectly homogeneous, (1.7) has solutions of the form $(11|\rho_\alpha^{(0)}) = \phi_\alpha(\mathbf{r})\exp(-i\Omega t - Dk_\alpha^2 t)$, where k_α is the spatial frequency of a solution to the wave equation $(\nabla^2 + k_\alpha^2)\phi_\alpha = 0$, with the boundary condition $\mathbf{n}\cdot\nabla\phi_\alpha = 0$. The eigenfunctions ϕ_α for a homogeneous field can serve as spatial basis states for a perturbative solution of the problem when $\nabla\Omega \neq 0$. The perturbative methods are described in Refs. [4], [6], and [7], which are generalizations of earlier work by Gamblin and Carver [10] and by Schearer and Walters [11], who developed theories of longitudinal spin relaxation in high-pressure gases due to magnetic-field inhomogeneities. Related studies of the effects of very large magnetic field inhomogeneities on spin relaxation have been reported by Barbé, Leduc, and Laloë [12] and Lefèvre-Seguin, Nacher, and Laloë [13]. McGregor [5] has shown that some of the perturbative expressions of Ref. [4] are identical to those that can be derived with Redfield theory [14].

From inspection of (1.7), we see that the perturbation described by the last two terms is the sum of a term proportional to $\nabla\Omega_z$, which mixes spatial states of the same transverse polarization $|11)$ into the unperturbed states, and a term proportional to $\nabla(\Omega_x - i\Omega_y)$, which admixes states of longitudinal polarization $|10)$. As the diffusion rate gets slower, the perturbative methods soon fail to describe the effects of $\nabla\Omega_z$, although they continue to account well for the effects of $\nabla(\Omega_x - i\Omega_y)$. The unperturbed damping rates, $\gamma_{\alpha,11} = -i\Omega + Dk_\alpha^2$, for states of the same transverse polarization $|11)$ have the same imaginary parts, but the separation of their real parts is of order D/h^2, where h is a characteristic linear dimension of the sample. Thus, the mixing amplitude for states of the same transverse polarization is on the order of

$$b = \frac{h^3}{D}\left|\frac{\partial\Omega_z}{\partial z}\right|. \tag{1.8}$$

If $\partial\Omega_z/\partial z \neq 0$, b will exceed unity if the diffusion coefficient D is sufficiently small, as it is in high-pressure gases and liquids. Perturbative methods fail when b is on the order of unity.

Here we want to consider the transition to the nonperturbative limit where $b \gg 1$. To simplify the subsequent discussion, we assume a long cylindrical cell, with the axis z of highest symmetry parallel to the homogeneous magnetic field, and with the top and bottom located at $z = \pm h$. The radius of the cylinder is relatively small, that is, $R \ll h$, so we neglect any dependence of the spin polarization on the x and y coordinates. Since the last term of (1.7) can be well accounted for by perturbation theory, we ignore it. We transform (1.7) to a dimensionless form by defining new spatial and temporal coordinates

$$\zeta = z/h \quad \text{and} \quad \tau = \frac{tD}{h^2}. \tag{1.9}$$

Denote the transverse spin polarization by $\psi(\zeta,\tau) = N(11|\rho)e^{i\Omega t}$, where N is a normalizing constant. The boundary condition (1.4) becomes

$$\frac{\partial\psi}{\partial\zeta} = 0 \quad \text{for} \quad \zeta = \pm1. \tag{1.10}$$

Finally, (1.7) becomes the *Torrey equation* [3],

$$\frac{\partial\psi}{\partial\tau} = \frac{\partial^2}{\partial\zeta^2}\psi + ib\zeta\psi. \tag{1.11}$$

II. SOLUTIONS FOR UNBOUNDED DIFFUSION

Consider the situation where the boundary condition (1.10) does not apply, and (1.11) is valid for all ζ. We seek a solution $\psi(\zeta,\tau)$ for times $\tau \geq 0$ in terms of $\psi(\zeta,0)$. Assume for the present that b is a non-negative real number. For notational convenience, we introduce new variables

$$x = b^{1/3}\zeta \quad \text{and} \quad t = b^{2/3}\tau \quad \text{and} \quad S(x,t) = \psi(\zeta,\tau). \tag{2.1}$$

This transforms (1.11) into

$$\frac{\partial S}{\partial t} = \frac{\partial^2 S}{\partial x^2} + ixS. \tag{2.2}$$

The Laplace transform of S is

$$\tilde{S}(x,s) = \int_0^\infty e^{-st} S(x,t)dt. \tag{2.3}$$

The inverse of (2.3) is

$$S(x,t) = \frac{1}{2\pi i}\int_V \tilde{S}(x,s)e^{st}ds. \tag{2.4}$$

The contour V is a vertical line in the complex s plane, located to the right of all singularities of the integrand. Substituting (2.3) into (2.2) we obtain the inhomogeneous differential equation

$$\left(s - ix - \frac{\partial^2}{\partial x^2}\right)\tilde{S}(x,s) = S(x,0). \tag{2.5}$$

The resolvent function $\tilde{G}(x,y,s)$ is the solution to the inhomogeneous differential equation

$$\left(s - ix - \frac{\partial^2}{\partial x^2}\right)\tilde{G}(x,y,s) = \delta(x-y). \tag{2.6}$$

We can use the resolvent to write the solution to (2.5) as

$$\tilde{S}(x,s) = \int_{-\infty}^\infty \tilde{G}(x,y,s)S(y,0)dy. \tag{2.7}$$

The inverse Laplace transform of (2.7) yields the solution in the time domain

$$S(x,t) = \int_{-\infty}^\infty G(x,y,t)S(y,0)dy, \tag{2.8}$$

where the Green's function G is the inverse Laplace transform of $\tilde{G}$. We will call kernels $G(x,y,t)$ *Green's functions* when they transform the initial spin polarization at position y and time $t = 0$ into the polarization at position x at a later time $t > 0$, and we will call kernels $\tilde{G}(x,y,s)$ *resolvents* when they produce the Laplace transform of the polarization.

To determine the resolvent, we introduce the function

$$f(ix-s,q) = \int_q^\infty e^{(ix-s)k-k^3/3}dk. \tag{2.9}$$

The lower limit of integration is an arbitrary complex number q, and the upper limit approaches infinity within the sextant of the complex k plane with $|\arg k| < \pi/6$, one of the three sextants where $e^{-k^3/3} \to 0$ as $|k| \to \infty$. Differentiating inside the integral sign gives

$$\begin{aligned}\left(s - ix - \frac{\partial^2}{\partial x^2}\right)f &= \int_q^\infty (s - ix + k^2)e^{(ix-s)k-k^3/3}dk \\ &= -\int_q^\infty d(e^{(ix-s)k-k^3/3}) \\ &= e^{(ix-s)q-q^3/3}.\end{aligned} \tag{2.10}$$

Equation (2.10) has a source term on the right-hand side which is nonzero for all finite values of x, q, and s. However, since (2.10) is linear, we can construct the resolvent by superposing functions f with different values of q,

$$\tilde{G}(x,y,s) = \frac{1}{2\pi}\int_{C_0} F\,dq, \tag{2.11}$$

where the integrand is

$$F = f(ix-s,q)\,e^{-(iy-s)q+q^3/3}. \tag{2.12}$$

We have designated the path of integration in the complex q plane by C_0, which, as sketched in Fig. 1(a), consists of the real axis from $-\infty$ to $+\infty$. Also sketched in Fig. 1(a) are other paths of integration, which will be useful in subsequent discussions. We shall show below that F approaches zero sufficiently rapidly as $q \to \pm\infty$ that (2.11) converges. In view of (2.10)– (2.12) we have

$$\begin{aligned}\left(s - ix - \frac{\partial^2}{\partial x^2}\right)\tilde{G}(x,y,s) &= \frac{1}{2\pi}\int_{-\infty}^\infty e^{iq(x-y)}dq \\ &= \delta(x-y),\end{aligned} \tag{2.13}$$

so (2.11) is indeed a solution of (2.6). The integrand F in (2.11) is analytic in the finite part of the complex q plane. We may therefore replace the path C_0 by either of the large semicircular paths $C_{\pm 1}$ sketched in Fig. 1(a). On the semicircles $|q| \gg 1$, so convenient asymptotic

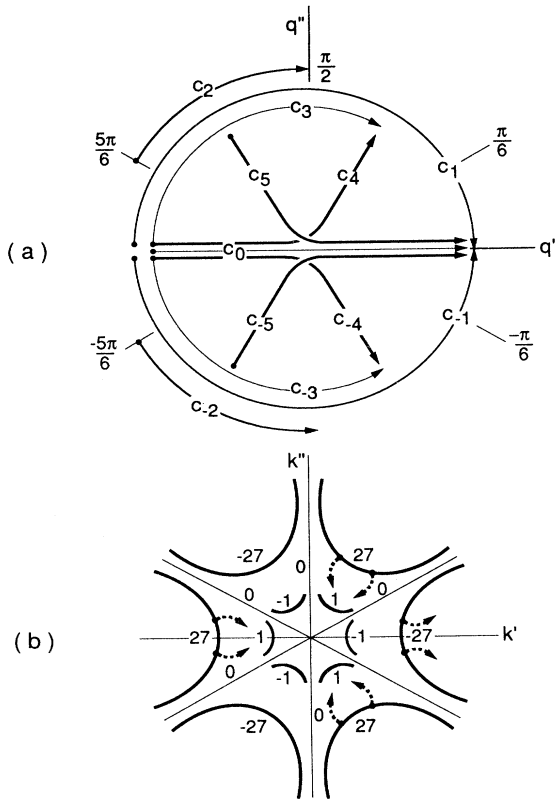

FIG. 1. (a) Integration paths in the complex q plane for evaluating the resolvent $\tilde{G}$ of (2.23). The paths begin and end at very large values of $|q|$. (b) On the solid lines in the complex k plane, $-\mathrm{Re}(k^3)$ has the values indicated. The dashed lines indicate paths of steepest descent on the surface $-\mathrm{Re}(k^3)$ from the initial values at $k = q$, indicated by the solid points. An asymptotic expression for the integral (2.9) can be obtained for the four sextants indicated to give the expression (2.15).

formulas can be used to express the integrand.

For sufficiently large values of $|q|$ the magnitude of the integrand of (2.9) will be dominated by the value of $-\mathrm{Re}(k^3)$ in the exponential. If we think of k' and k'', the real and imaginary components of k, as orthogonal coordinates, then $-\mathrm{Re}(k^3)$ is a harmonic function, which has the same altitude contours as a membrane stretched on a circular rim whose height above the k',k'' plane varies as $-\cos 3\theta$, where θ is the azimuthal angle on the plane. From inspection of (2.9) we see that for large $|q|$, most of the value of the integral comes from the segment of path near the maximum of $-\mathrm{Re}(k^3)$. If the path of integration can be chosen such that $-\mathrm{Re}(k^3)$ decreases steeply and monotonically from a relatively large initial value, we can get an asymptotic approximation to (2.9) by integrating for a short distance in the direction of steepest descent of $-\mathrm{Re}(k^3)$. As sketched in Fig. 1(b), such paths exist for all large values of $|q|$ outside the two sextants

$$\pi/2 < |\arg q| < 5\pi/6. \tag{2.14}$$

Outside the sextants (2.14), integration of (2.9) along the direction of steepest descent transforms (2.12) to

$$F \sim e^{i(x-y)q}\int_0^\infty e^{-q^2t}dt = \frac{1}{q^2}e^{i(x-y)q}. \tag{2.15}$$

We see from this expression that for large $|q|$, F is exponentially small in the upper half of the q plane if $x > y$, and exponentially small in the lower half of the q plane if $x < y$. Also, F approaches zero rapidly enough as $q \to \pm\infty$ along the real axis that (2.11) converges.

Now consider values of q in the sextants (2.14) where (2.15) is not valid, since the path of integration must go uphill and cross a ridge on the surface $-\mathrm{Re}(k^3)$ before going downhill again. For large values of $|q|$ in the sextants (2.14), the integrand of (2.9) is vanishingly small so f is independent of q. Furthermore, the right-hand side of (2.10) approaches zero, and f becomes a solution of the homogeneous differential equation $(s-ix-\partial^2/\partial x^2)f = 0$. With the change of variables $w = ix-s$ and $f(ix-s,q) = \chi(w)$, this becomes Airy's differential equation [15, 16] $\chi'' = w\chi$. Since we will frequently be concerned with the characteristic threefold symmetry of Airy functions [if $\chi(w)$ is a solution of Airy's differential equation, then $\chi(e^{\pm 2\pi i/3}w)$ is also a solution], it will be convenient to denote the angle for a third of a turn about the circle by

$$\alpha = \frac{2\pi}{3}. \tag{2.16}$$

From the well-known integral expressions of the Airy functions [16] we find for large values of $|q|$ in the sextants (2.14)

$$f \to \int_{C_5} e^{(ix-s)k-k^3/3}dk = 2\pi i\, e^{-i\alpha}\mathrm{Ai}(e^{-i\alpha}(ix-s))$$

$$\text{as } |q| \to \infty \quad \text{with} \quad \pi/2 < \arg q < 5\pi/6. \tag{2.17}$$

Similarly,

$$f \to \int_{C_{-5}} e^{(ix-s)k-k^3/3}dk = -2\pi i\, e^{i\alpha}\mathrm{Ai}(e^{i\alpha}(ix-s))$$

$$\text{as } |q| \to \infty \quad \text{with} \quad -\pi/2 > \arg q > -5\pi/6. \tag{2.18}$$

Consider the case $x > y$, and let us evaluate $\tilde{G}$ according to (2.11) on the upper semicircular path C_1. According to (2.15), F is negligibly small on C_1 unless $\pi/2 < \arg q < 5\pi/6$. From (2.12) and (2.17), the asymptotic value of F in this sextant is

$$F = 2\pi i\, e^{-i\alpha}\mathrm{Ai}(e^{-i\alpha}(ix-s))e^{-(iy-s)q+q^3/3}. \tag{2.19}$$

Thus, the resolvent (2.11) is

$$\begin{aligned}\tilde{G}(x,y,s) &= \frac{1}{2\pi}\int_{C_1} F dq \\ &= ie^{-i\alpha}\mathrm{Ai}(e^{-i\alpha}(ix-s)) \\ &\quad\times \int_{C_2} e^{-(iy-s)q+q^3/3}dq.\end{aligned} \tag{2.20}$$

Since the integrand F is negligibly small outside the sextant $\pi/2 < \arg q < 5\pi/6$, we have replaced C_1 by C_2, and we have used (2.19) to factor out the Airy function. Since $e^{-(iy-s)q+q^3/3}$ is negligibly small for the parts of C_3 that extend beyond C_2, we can also write

$$\begin{aligned}\int_{C_2} e^{-(iy-s)q+q^3/3}dq &= \int_{C_3} e^{-(iy-s)q+q^3/3}dq \\ &= \int_{C_4} e^{-(iy-s)q+q^3/3}dq.\end{aligned} \tag{2.21}$$

The last equality is true because the integrand is analytic in the finite q plane, and the paths C_3 and C_4 begin and end at the same points. Setting $k = -q$ in (2.21) and using (2.18) we find

$$\begin{aligned}\int_{C_4} e^{-(iy-s)q+q^3/3}dq &= \int_{C_{-5}} e^{(iy-s)k-k^3/3}dk \\ &= -2\pi i\, e^{i\alpha}\mathrm{Ai}(e^{i\alpha}(ix-s)).\end{aligned} \tag{2.22}$$

Using this in (2.20) we have

$$\tilde{G}(x,y,s) = 2\pi\mathrm{Ai}(e^{-i\alpha}(ix-s))\mathrm{Ai}(e^{i\alpha}(iy-s)) \quad \text{if} \quad x > y. \tag{2.23a}$$

For $x < y$ we may replace C_0 in (2.11) with the lower semicircle C_{-1} and proceed as above to find

$$\tilde{G}(x,y,s) = 2\pi\mathrm{Ai}(e^{i\alpha}(ix-s))\mathrm{Ai}(e^{-i\alpha}(iy-s)) \quad \text{if} \quad x < y. \tag{2.23b}$$

In subsequent sections, we will denote the resolvent (2.23) by $\tilde{G}_0$ to distinguish it from related resolvents with one or two boundaries.

To find the Green's function that appears in (2.8) we introduce new variables t and r defined by

$$q = \frac{r-t}{2} \qquad \text{and} \qquad k = \frac{r+t}{2}. \tag{2.24}$$

Then (2.11) becomes

$$\tilde{G}(x,y,s) = \tfrac{1}{4\pi}\int_0^\infty dt\; e^{-ts+it(x+y)/2-t^3/12} \times \left(\int_{-\infty}^{\infty} dr\, e^{ir(x-y)/2-r^2t/4}\right) = \int_0^\infty dt\, \frac{1}{\sqrt{4\pi t}} e^{-(x-y)^2/4t+it(x+y)/2-t^3/12-st}. \tag{2.25}$$

Comparing this with the definition of the Laplace transform, cf. (2.3), we see that

$$G(x,y,t) = \frac{1}{\sqrt{4\pi t}} \exp\left(-\frac{(x-y)^2}{4t} + \frac{it(x+y)}{2} - \frac{t^3}{12}\right). \tag{2.26}$$

We define the spatial Fourier transform of the resolvent by

$$\tilde{P}(k,q,s) = \frac{1}{2\pi}\int e^{-i(kx-qy)}\tilde{G}(x,y,s)dx\,dy. \tag{2.27}$$

The inverse of (2.27) is

$$\tilde{G}(x,y,s) = \frac{1}{2\pi}\int e^{i(kx-qy)}\tilde{P}(k,q,s)dk\,dq. \tag{2.28}$$

From inspection of (2.28), (2.9), (2.11), and (2.12) we recognize that

$$\tilde{P}(k,q,s) = \eta(k-q)\exp[-\tfrac{1}{3}(k^3-q^3) - s(k-q)], \tag{2.29}$$

where η is the Heaviside unit-step function

$$\eta(x) = \begin{cases} 1 & \text{if } x \geq 0 \\ 0 & \text{if } x < 0. \end{cases} \tag{2.30}$$

The momentum-space Green's function is given by the inverse Laplace transform of (2.29). We may use the well-known identity $\int_V e^{sx}ds = 2\pi i\delta(x)$ and note that $t \geq 0$ to find

$$P(k,q,t) = \delta(k-q-t)\exp[-\tfrac{1}{3}(k^3-q^3)]. \tag{2.31}$$

To discuss the physical significance of these results, we reintroduce the variables ζ and τ and the parameter b in accordance with (2.1). We denote the functions for the two sets of variables with the same letters G and P. The context will indicate which set of variables is understood. Then (2.26) becomes

$$G(\zeta,\xi,\tau) = b^{1/3}G(x,y,t) = \frac{1}{\sqrt{4\pi\tau}}\exp\left(-\frac{(\zeta-\xi)^2}{4\tau} + \frac{ib\tau(\zeta+\xi)}{2} - \frac{b^2\tau^3}{12}\right). \tag{2.32}$$

Physically, (2.32) describes the transverse spin polarization, observed at the position ζ and time τ, generated by a point source of transverse spin, located at the position ξ at time $\tau = 0$. If $b = 0$, the Torrey equation (1.11) reduces to the equation for heat conduction in one dimension, and (2.33) becomes the well-known [17] space-time dependence of a heat-pole. For nonzero b, the behavior is similar to heat diffusion, but at an observation point ζ the polarization precesses at the average of the Larmor frequencies $b\xi$ and $b\zeta$ at the source and observation points, and the polarization damps exponentially with τ^3. Note that

$$G(\zeta,\xi,\tau) \to \delta(\zeta-\xi) \qquad \text{as} \qquad \tau \to 0. \tag{2.33}$$

For a uniform initial polarization, $\psi(\zeta,0) = 1$, the polarization evolves to

$$\psi(\zeta,\tau) = \int_{-\infty}^{\infty} G(\zeta,\xi,\tau)\psi(\xi,0)d\xi = \exp\left(ib\zeta\tau - b^2\tau^3/3\right), \tag{2.34}$$

from which Hahn's formula (1.1) follows.

To reintroduce b to the formulas for momentum space and the resolvents, we make the change of variables

$$k = \kappa b^{-1/3} \qquad \text{and} \qquad q = \rho b^{-1/3}. \tag{2.35}$$

The momentum-space Green's function (2.31) becomes

$$P(\kappa,\rho,\tau) = b^{-1/3}P(k,q,t) = \delta(\kappa-\rho-b\tau)\exp\left(-\frac{1}{3b}(\kappa^3-\rho^3)\right). \tag{2.36}$$

According to (2.36), a component of the wave function with initial momentum (spatial frequency) ρ will evolve into a component with momentum $\kappa = \rho + b\tau$ at time τ, and will have been damped by the factor $\exp[(\rho^3-\kappa^3)/3b]$. Physically, an initially positive spatial frequency $\rho > 0$, that is, a right-handed spiral of spins, will increase, because the field inhomogeneity twists the transverse spin polarization into ever tighter spirals. The damping is caused by diffusion of spins across the half-period distances π/κ of the instantaneous spatial frequency κ. If the initial spatial frequency is negative, $\rho < 0$, the field inhomogeneity will first unwind the left-handed spiral and then wind the spins into a right-handed spiral with an increasingly positive spatial frequency.

The double line integral (2.11) permits one to obtain four kernels: space time (2.26), space frequency (2.23), momentum time (2.31), and momentum frequency (2.29). Alternatively, all of the kernels can be derived directly by solving differential equations with appropriate boundary conditions, but it is hard to show directly that (2.23) and (2.26) are Laplace-transform pairs and that (2.23) and (2.29) are Fourier-transform pairs.

III. ONE NONDEPOLARIZING BOUNDARY

Suppose there is a nondepolarizing boundary at $x = l$ so that the resolvent (2.6) satisfies the boundary condition

$$\frac{\partial\tilde{G}}{\partial x}(x,y,s) = 0 \qquad \text{at} \qquad x = l. \tag{3.1}$$

For convenience, we make the change of variable

$$w = ix - s \qquad \text{with} \qquad \chi(w) = \tilde{G}(x,y,s), \tag{3.2}$$

and we think of y as a fixed parameter. Then for $x \neq y$, (2.6) becomes Airy's differential equation

$$\chi'' = w\chi, \tag{3.3}$$

where the prime denotes differentiation with respect to w. Any pair of the Airy functions $\mathrm{Ai}(w)$, $\mathrm{Ai}(e^{-i\alpha}w)$, or $\mathrm{Ai}(e^{i\alpha}w)$ can be used to express the general solution of (3.3), so we write

$$\chi(w) = \begin{cases} A\mathrm{Ai}(e^{-i\alpha}w) + B\mathrm{Ai}(e^{i\alpha}w) & \text{if } x < y \\ C\mathrm{Ai}(e^{-i\alpha}w) + D\mathrm{Ai}(e^{i\alpha}w) & \text{if } x > y. \end{cases} \tag{3.4}$$

Note that

$$\text{as } x \to \infty, \quad \mathrm{Ai}(e^{-i\alpha}w) \to 0 \quad \text{and} \quad \mathrm{Ai}(e^{i\alpha}w) \to \infty; \tag{3.5}$$

$$\text{as } x \to -\infty, \quad \mathrm{Ai}(e^{-i\alpha}w) \to \infty \quad \text{and} \quad \mathrm{Ai}(e^{i\alpha}w) \to 0. \tag{3.6}$$

Suppose that the diffusion is bounded on the left at l. Then we are interested in solutions of (2.6) that satisfy (3.1) and for which $x \geq l$ and $y \geq l$. For finite values of y and s we must have

$$\tilde{G}(x, y, s) \to 0 \qquad \text{as} \qquad x \to \infty. \tag{3.7}$$

We conclude from (3.5) and (3.7) that

$$D = 0. \tag{3.8}$$

From (3.1) and (3.4) we see that

$$A\, ie^{-i\alpha}\mathrm{Ai}'(e^{-i\alpha}w_l) + B\, ie^{i\alpha}\mathrm{Ai}'(e^{i\alpha}w_l) = 0, \tag{3.9}$$

where

$$w_l = il - s. \tag{3.10}$$

The δ function in (2.6) produces a unit discontinuity in the slope of $\tilde{G}$ at $x = y$, so (3.4) implies

$$1 = A\, ie^{-i\alpha}\mathrm{Ai}'(e^{-i\alpha}w_y) + B\, ie^{i\alpha}\mathrm{Ai}'(e^{i\alpha}w_y) - C\, ie^{-i\alpha}\mathrm{Ai}'(e^{-i\alpha}w_y), \tag{3.11}$$

where

$$w_y = iy - s. \tag{3.12}$$

Since $\tilde{G}'$ is continuous except for the unit discontinuity at $x = y$, $\tilde{G}$ must be continuous for all $x \geq l$, including $x = y$, so we write

$$A\,\mathrm{Ai}(e^{-i\alpha}w_y) + B\,\mathrm{Ai}(e^{i\alpha}w_y) - C\,\mathrm{Ai}(e^{-i\alpha}w_y) = 0. \tag{3.13}$$

Solving the simultaneous equations (3.9), (3.11), and (3.13) for the coefficients A, B, and C, and substituting these values into (3.4), we obtain the resolvent for diffusion to the right of a nondepolarizing boundary at $x = l$

$$\tilde{G} = \tilde{G}_0 + \tilde{G}_1, \tag{3.14}$$

where $\tilde{G}_0$, the resolvent for unbounded diffusion, is given by (2.23), and the correction due to the boundary is

$$\tilde{G}_1 = -\,2\pi e^{2i\alpha}\mathrm{Ai}'(e^{i\alpha}(il - s))\mathrm{Ai}(e^{-i\alpha}(ix - s)) \times \mathrm{Ai}(e^{-i\alpha}(iy - s))/\mathrm{Ai}'(e^{-i\alpha}(il - s)). \tag{3.15}$$

Note that

$$\tilde{G}_1 \to 0 \qquad \text{as} \qquad l \to -\infty. \tag{3.16}$$

The Wronskian [19]

$$\frac{e^{i3\alpha/4}}{2\pi} = e^{-i\alpha}\mathrm{Ai}(e^{i\alpha}z)\mathrm{Ai}'(e^{-i\alpha}z) - e^{i\alpha}\mathrm{Ai}'(e^{i\alpha}z)\mathrm{Ai}(e^{-i\alpha}z) \tag{3.17}$$

was used to simplify (3.14) and (3.15). Equation (3.17) is valid for any complex number z. For future reference, we note that (3.17) remains valid if we substitute $-\alpha$ for α. We see from (3.15) that the resolvent (3.14) has simple poles when

$$\mathrm{Ai}'(e^{-i\alpha}(il - s)) = 0, \tag{3.18}$$

that is, when

$$s = s_{n\alpha} = il - a_n' e^{i\alpha} \qquad \text{for } n = 1, 2, 3, \ldots, \tag{3.19}$$

where a_n' is one of the zeros of the entire function Ai'. The a_n' are negative real numbers [15]. In order of increasing magnitude the first three are $a_1' = -1.018\,792\,97$, $a_2' = -3.248\,197\,58$, $a_3' = 4.820\,099\,21$. The poles recede to $-i\infty$ when $l \to -\infty$, as one would expect, since the resolvent for unbounded diffusion has no poles in the finite s plane.

The residue of the resolvent (3.14) at $s = s_{n\alpha}$ is readily shown to be

$$\lim_{s \to s_{n\alpha}} (s - s_{n\alpha})\tilde{G}(x, y, s) = N_{n\alpha}^2 \mathrm{Ai}(e^{-i\alpha}(ix - s_{n\alpha})) \times \mathrm{Ai}(e^{-i\alpha}(iy - s_{n\alpha})). \tag{3.20}$$

The normalization coefficient is

$$N_{n\alpha}^2 = \frac{1}{e^{7i\alpha/4}\, a_n' \mathrm{Ai}^2(a_n')}. \tag{3.21}$$

The Wronskian (3.17) was used to simplify these expressions. The Airy functions of (3.20) are solutions of the homogeneous version of (2.6),

$$\left(s_{n\alpha} - ix - \frac{\partial^2}{\partial x^2}\right) \mathrm{Ai}(e^{-i\alpha}(ix - s_{n\alpha})) = 0. \tag{3.22}$$

The Airy functions of (3.22) satisfy the boundary conditions

$$\mathrm{Ai}' = 0 \quad \text{when} \quad x = l; \qquad \mathrm{Ai} \to 0 \quad \text{as} \quad x \to \infty. \tag{3.23}$$

Multiplying (3.22) on the left-hand side by the eigenfunction for $s_{m\alpha}$ and integrating, one can readily verify that

$$N_{n\alpha}N_{m\alpha}\int_l^\infty \mathrm{Ai}(e^{-i\alpha}(ix - s_{n\alpha}))\mathrm{Ai}(e^{-i\alpha}(ix - s_{m\alpha}))dx = \delta_{nm}. \tag{3.24}$$

To verify the normalization explicitly, one can make use of (10.4.57) of Ref. [15]. In analogy with (2.4), the Green's function is the inverse Laplace transform of the

resolvent

$$G = \frac{1}{2\pi i}\int_V \tilde{G}e^{st}ds$$
$$= \sum_{n=1}^{\infty} N_{n\alpha}^2 \mathrm{Ai}(e^{-i\alpha}(ix - s_{n\alpha}))\mathrm{Ai}(e^{-i\alpha}(iy - s_{n\alpha}))$$
$$\times \exp(s_{n\alpha}t). \qquad (3.25)$$

Thus, the Green's function (3.25) for a nondepolarizing boundary on the left at $x = l$ can be conveniently expressed as an eigenfunction expansion. Since the operator in (3.22) is not Hermitian, the eigenvalues $s_{n\alpha}$ are complex instead of real, and there is no complex conjugate symbol on either of the eigenfunctions in the orthogonality relation (3.24). According to (3.19), the real parts of the eigenvalues are all negative, so (3.25) is a sum of damped oscillations with respect to time. The eigenfunctions span a complex orthogonal space rather than a unitary space, and the eigenvalues are said to be rectanormal. Schneider and Freed [18] have given an excellent review of the basic properties of such spaces, which occur naturally in the discussion of many kinds of spin relaxation.

For diffusion bounded on the right, we require $x \leq l$ and $y \leq l$. We must replace α by $-\alpha$ in (3.14)–(3.25). Additional modifications are in (3.16), $\tilde{G}_1 \to 0$ as $l \to \infty$; in (3.23), Ai $\to 0$ as $x \to -\infty$; in (3.24), the integral extends from $-\infty$ to l. Sketched in Fig. 2 are the eigenvalues $s_{n,\pm\alpha}$ for diffusion to the right and to the left of a boundary.

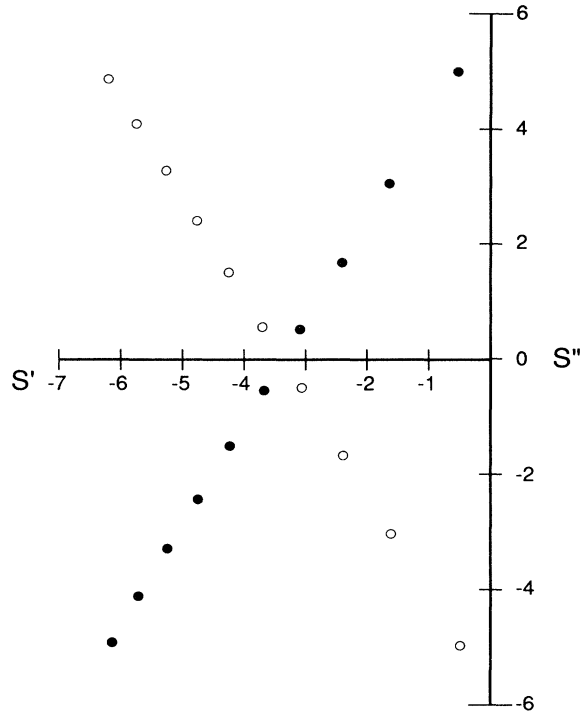

FIG. 2. Pole locations in the complex s plane of the resolvent (3.14) for a single nondepolarizing boundary. Open circles: $s_{n,\alpha}$ for diffusion to the right of a boundary located at $x = -(200)^{1/3}$. Solid circles: $s_{n,-\alpha}$ for diffusion to the left of a boundary located at $x = (200)^{1/3}$.

IV. TWO NONDEPOLARIZING BOUNDARIES

The first analysis of the Torrey equation ($b \neq 0$) with two nondepolarizing boundaries seems to be that of Robertson [19], who obtained approximate solutions, with qualitatively correct limiting decay rates for slow and fast diffusion, but with a range of validity which is hard to estimate. Freed [20] and his colleagues, in their analysis of spin waves in polarized atomic hydrogen, showed that the eigenfunctions are Airy functions. They made extensive numerical studies of the solutions, and they showed that these solutions provide a good description of spin-wave experiments. We will discuss the problem from several viewpoints: first, as an extension of the previous discussion of unbounded diffusion and diffusion with one nondepolarizing boundary; secondly, by means of direct numerical integration of the Torrey equation; and finally, in terms of an abstract vector space.

Suppose there are nondepolarizing boundaries at $x = \pm l$ so that

$$\frac{\partial \tilde{G}}{\partial x}(x, y, s) = 0 \qquad \text{at} \qquad x = \pm l, \qquad (4.1)$$

and let $-l \leq x \leq l$ and $-l \leq y \leq l$. The same considerations apply as in the discussion of one boundary. The four coefficients A, B, C, and D of (3.4) are determined by the two conditions (4.1), by the requirement that $\tilde{G}$ have a unit discontinuity at $x = y$, which gives an equation analogous to (3.11), and by the requirement that $\tilde{G}$ be continuous at $x = y$, which gives an equation analogous to (3.13). The resolvent is

$$\tilde{G} = \tilde{G}_0 + \tilde{G}_1, \qquad (4.2)$$

where the correction to the resolvent $\tilde{G}_0$ for unbounded diffusion is

$$\tilde{G}_1 = \frac{1}{\Delta}\mathrm{Ai}'(e^{i\alpha}w_-)\mathrm{Ai}'(e^{-i\alpha}w_+)\left[\mathrm{Ai}(e^{-i\alpha}w_x)\mathrm{Ai}(e^{i\alpha}w_y) + \mathrm{Ai}(e^{i\alpha}w_x)\mathrm{Ai}(e^{-i\alpha}w_y)\right]$$
$$-\frac{1}{\Delta}e^{2i\alpha}\mathrm{Ai}'(e^{i\alpha}w_-)\mathrm{Ai}(e^{i\alpha}w_+)\mathrm{Ai}(e^{-i\alpha}w_x)\mathrm{Ai}(e^{-i\alpha}w_y)$$
$$-\frac{1}{\Delta}e^{-2i\alpha}\mathrm{Ai}'(e^{-i\alpha}w_-)\mathrm{Ai}(e^{-i\alpha}w_+)\mathrm{Ai}(e^{i\alpha}w_x)\mathrm{Ai}(e^{i\alpha}w_y), \qquad (4.3)$$

where the denominator is the entire function

$$\Delta(s,l)=\frac{1}{2\pi}[\ \mathrm{Ai}'(e^{-i\alpha}w_-)\mathrm{Ai}'(e^{i\alpha}w_+) -\mathrm{Ai}'(e^{i\alpha}w_-)\mathrm{Ai}'(e^{-i\alpha}w_+)], \tag{4.4}$$

and where

$$w_\pm=\pm il-s; \qquad w_x=ix-s; \qquad w_y=iy-s. \tag{4.5}$$

The resolvent has poles at the values $s=s_n$ for which

$$\Delta(s_n,l)=0. \tag{4.6}$$

There are infinitely many first-order poles, as in the case discussed above of a single boundary. In addition, there are second order poles for exceptional values of l. Numerical studies show no evidence for higher-order poles.

A. Numerical studies

Much insight can be gained from numerical studies of the Torrey equation. We investigate solutions that decay exponentially with the first power of the time,

$$\psi(\zeta,\tau)=\phi(\zeta)e^{-\gamma\tau}\ . \tag{4.7}$$

Substituting (4.7) into (1.11) we obtain the *time-independent Torrey equation*

$$\left(\gamma+ib\zeta+\frac{\partial^2}{\partial\zeta^2}\right)\phi=0, \tag{4.8}$$

where ϕ must satisfy the boundary conditions

$$\frac{\partial\phi}{\partial\zeta}(\zeta)=0 \qquad \text{at} \qquad \zeta=\pm1. \tag{4.9}$$

Solutions of (4.8) satisfying (4.9) exist only for discrete eigenvalues γ_n. We can more clearly understand the dependence of γ_n on b if we think of b as an arbitrary complex number. The eigenvalues γ_n of (4.8) are branches, interconnected at branch points, of the multivalued function $\gamma(b)$. For ordinary magnetic resonance applications of the Torrey equation (1.11), the parameter b will be a real number, but an imaginary component of b is conceivable. It could correspond to a local relaxation mechanism that varied linearly along the cell axis. A gradient in the chemical composition or temperature could cause such a dependence. If b is purely imaginary, (4.8) becomes the time-independent Schrödinger equation for a particle of fixed energy, $E\propto\gamma$, subject to a constant force, $F\propto b$, in the ζ direction. When written in terms of ζ, τ, and b, the expressions for Green's functions and resolvents of Sec. II and III remain formally correct for complex values of b. For some complex values of b, however, the solutions grow without limit as time increases.

For $b=0$, the Torrey equation (1.11) with the boundary condition (1.10) reduces to the equation of heat conduction on a thin ring with a circumference of two units. Sommerfeld [17] shows that for this case the Green's function G is the sum of two ϑ functions. For $b=0$ the solutions of (4.8) are simply

$$\phi_n(\zeta)=\cos n\pi(\zeta+1)/2 \quad \text{for } n=0,1,2,\ldots\ . \tag{4.10}$$

The eigenvalues are

$$\gamma_{n0}=\frac{n^2\pi^2}{4}. \tag{4.11}$$

For sufficiently small values of b, the eigenvalue γ_n can be expressed as a power series in b; that is

$$\gamma_n=\frac{n^2\pi^2}{4}+k_2b^2+k_4b^4+\cdots, \tag{4.12}$$

where the coefficients k_2, $k_4,\ldots$, depend on n. For example, using the perturbation methods of Refs. [4], [6], and [7], one can readily show that

$$\gamma_0=\frac{2b^2}{15}+\cdots. \tag{4.13}$$

Multiplying (4.8) for the nth eigenfunction ϕ_n by the complex conjugate ϕ_n^* and integrating by parts over the interval [-1,1] with the boundary conditions (4.9) gives

$$\gamma_n=\left(\int_{-1}^{1}|\phi_n'|^2-ib\int_{-1}^{1}|\phi_n|^2\zeta\,d\zeta\right)\left(\int_{-1}^{1}|\phi_n|^2d\zeta\right)^{-1}. \tag{4.14}$$

We see from (4.14) that for real values of b, the real part of the eigenvalue γ_n must be non-negative, while for purely imaginary values of b, γ_n will be real, which must be so since (4.8) is then Hermitian.

Suppose that (4.8), with the boundary conditions (4.9), is satisfied for the parameter b_{n1}, an eigenvalue γ_{n1}, and an eigenfunction ϕ_{n1}. Then the symmetry of (4.8) implies that there are three other solutions ϕ_{nm} for $m=2,3,4$, corresponding to inhomogeneity parameters $b=b_{nm}$ and eigenvalues γ_{nm}, as listed in Table I.

There can be no more than one linearly independent solution of (4.8) with the boundary condition (4.9). Thus, if b_{n1} and γ_{n1} are real, we must have $\phi_{n1}^*(-\zeta)\propto\phi_{n1}(\zeta)$, and we can always choose ϕ_{n1} such that

$$\phi_{n1}^*(\zeta)=\phi_{n1}(-\zeta). \tag{4.15}$$

Starting with the identity

$$\int_{-1}^{1}\phi_m\left(\gamma_n+ib\zeta+\frac{d^2}{d\zeta^2}\right)\phi_n\,d\zeta=0, \tag{4.16}$$

which follows from (4.8), integrating by parts, and using (4.9), one can show that

$$(\gamma_m-\gamma_n)\int_{-1}^{1}\phi_m\phi_n d\zeta=0. \tag{4.17}$$

Thus, $\int_{-1}^{1}\phi_m\phi_n\,d\zeta=0$ if $\gamma_m\neq\gamma_n$.

We have used a Runge-Kutta algorithm [21] to integrate (4.8) from $\zeta=-1$ to $\zeta=+1$ with the initial condition

$$\phi(-1)=1 \qquad \text{and} \qquad \phi'(-1)=0. \tag{4.18}$$

TABLE I. Symmetry relations among solutions of the time-independent Torrey equation.

m	b_{nm}	$\phi_{nm}(\zeta)$	γ_{nm}
1	b_{n1}	$\phi_{n1}(\zeta)$	γ_{n1}
2	$-b_{n1}$	$\phi_{n1}(-\zeta)$	γ_{n1}
3	b^*_{n1}	$\phi^*_{n1}(-\zeta)$	γ^*_{n1}
4	$-b^*_{n1}$	$\phi^*_{n1}(\zeta)$	γ^*_{n1}

Values of $\phi'(1)$ were computed for two trial values of γ, and several iterations of the secant method [21] were used to find the values of γ for which $\phi'(1) = 0$, in accordance with the boundary condition (4.9). As shown in Fig. 3, as b increases along the positive real axis, successive pairs of eigenvalues coalesce at branch points $b = B_1, B_2, B_3, \ldots$, to common values $\Gamma_1, \Gamma_2, \Gamma_3, \ldots$. In Sec. VI we show that the positive, real values of b and γ at the branch points are related by

$$B_p = \sqrt{3}\Gamma_p. \tag{4.19}$$

The first few B_p, calculated from the zeros j_p of the Bessel function $J_{-2/3}$ in accordance with the formula (6.20) derived below, are listed in Table II. There is no difference, within computational accuracy, between the branch points found by numerical solution of (4.8) and the values from (6.20).

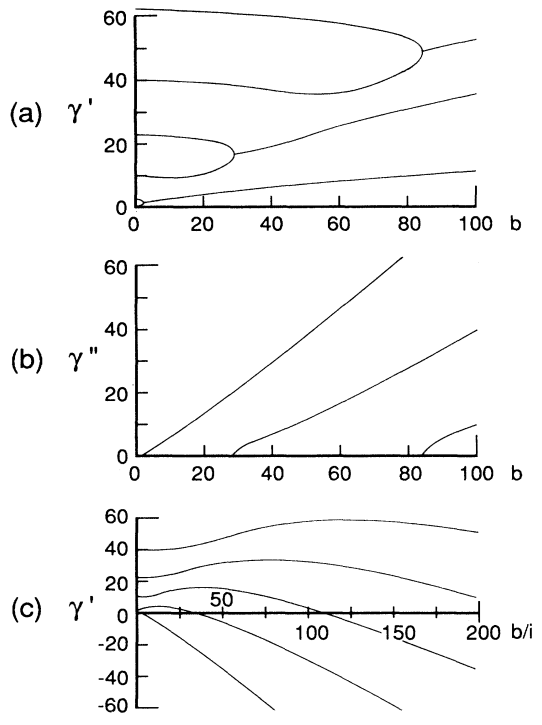

FIG. 3. (a) The real parts of the eigenvalues of the time-independent Torrey equation (4.8) for diffusion between two nondepolarizing boundaries. (b) The imaginary parts of the eigenvalues above. There are infinitely many branch points on the real b axis. (c) The eigenvalues of (4.8) for imaginary b; all eigenvalues are real and there are no branch points.

TABLE II. Zeros of $J_{-2/3}$ and corresponding branch points.

p	j_p	B_p
1	1.243 04	2.2581
2	4.429 12	28.669
3	7.579 45	83.956
4	10.724 74	168.09
5	13.868 37	281.08
6	17.011 25	422.91
7	20.153 73	593.59

In view of the symmetry properties of Table I, there are also branch points on the negative real axis at $-B_1, -B_2, -B_3, \ldots$. Also shown in Fig. 3 is the dependence of the eigenvalues on purely imaginary b. There are no branch points on the imaginary axis, but there are branch points above and below the real axis of the complex b plane. The mapping of two sheets of the b plane onto one sheet of the γ plane near the first complex branch point is shown in Fig. 4.

For large real values of b, many eigenvalues are complex. A plot of the eigenvalues in the complex γ plane is shown in Fig. 5 for $b = 200$. Note that the eigenvalues lie very nearly on a trigon, which intercepts the imaginary γ axis at $\pm ib$ and has a vertex on the real axis at $b/\sqrt{3}$.

The qualitative behavior of the eigenfunctions ϕ_n is sketched in Fig. 6. We have represented the eigenfunctions $\phi_n(\zeta)$ in the space ξ, η, ζ with $\xi = \mathrm{Re}(\phi_n)$ and $\eta = \mathrm{Im}(\phi_n)$. For esthetic reasons, we chose a left-handed coordinate system, so the sketches correspond to a field gradient which twists the spin polarization into a left-handed screw. The eigenfunction of Fig. 6(a), ϕ_0 for $b = 400$, is localized near the left boundary; the damping rate γ is complex and has a relatively small real part. The eigenfunction of Fig. 6(b), ϕ_6 for $b = 400$, is localized on the left-hand side of the interval; it has a complex damping rate with a larger real part. The eigenfunction of Fig. 6(c), ϕ_{12} for $b = 400$, is centered in the interval and has a purely real damping rate, but it is still strongly perturbed and localized with respect to the function it evolves from in the limit of no field inhomogeneity. The eigenfunction of Fig. 6(d), ϕ_{10} with $b = 2$, is delocalized and has a damping rate that differs only slightly from the value (4.11) for no field inhomogeneity. It differs from the sinusoids of (4.10) by not quite lying in the ξ-ζ plane. The eigenfunctions of Figs. 6(a) and 6(b) are almost identical to the eigenfunctions of Sec. III for a single nondepolarizing boundary. The eigenvalue equations (3.22) and (4.8) are identical if we make the substitution (2.1) with $\gamma = -b^{2/3}s_n$. If the eigenfunction is vanishingly small at one of the two boundaries, then the conditions (4.9) for two boundaries have the same effect as the conditions (3.23) for one boundary. Thus, (3.19) implies that the complex eigenvalues should be given very nearly by

$$\gamma_n = \pm ib + b^{2/3}a'_n e^{\pm i\alpha} \quad \text{for} \quad n = 1, 2, 3, \ldots. \tag{4.20}$$

Equation (4.20) works for complex as well as real values

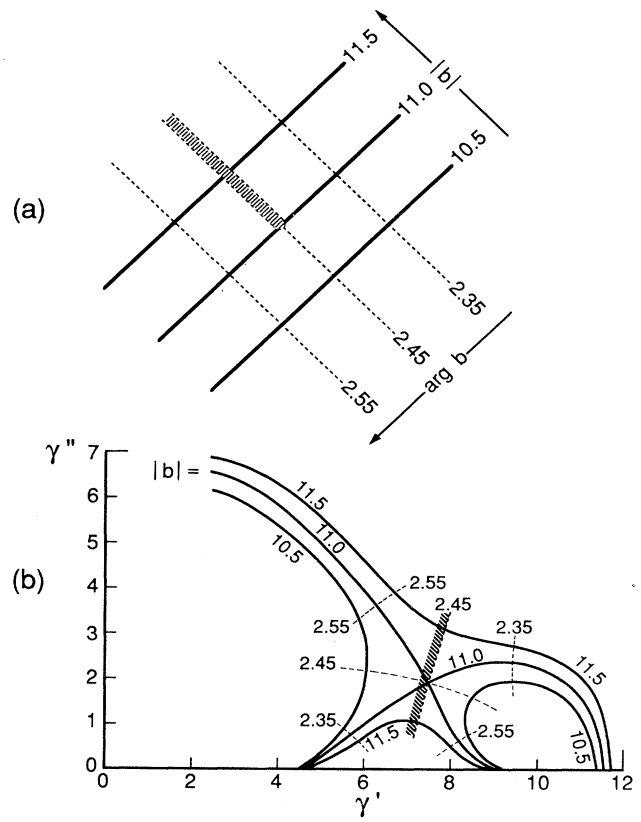

FIG. 4. (a) Arcs of constant $|b|$ and rays of constant $\arg b$ in the neighborhood of the branch point with $|B| = 10.991$ and $\arg B = 2.452$ in the complex b plane. (b) The mapping of the rays and arcs of (a) onto the γ plane. The cut outward along a ray through the branch point in the b plane keeps the mapping one-to-one. Since the branch point is second order, a circuit from one edge of the cut in the b plane, around the branch point to the adjacent point on the other edge carries the corresponding value of γ to the opposite side of the branch point, located at $\Gamma = 7.76 + 1.98i$. The mappings near other real and complex branches are similar (cf. Fig. 7).

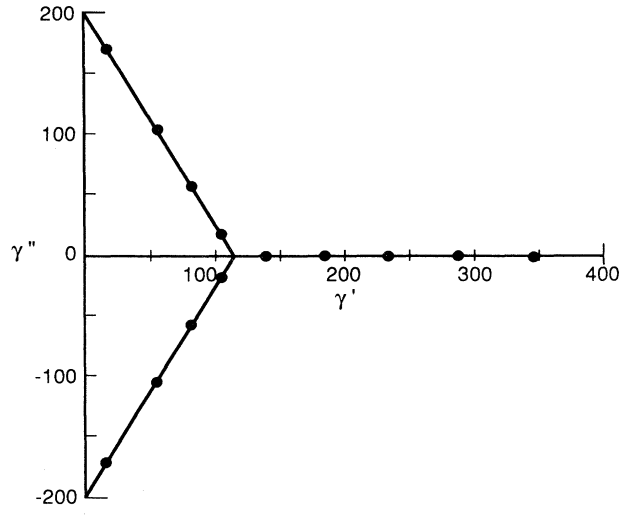

FIG. 5. Eigenvalues of the time-independent Torrey equation (4.8) for $b = 200$. The complex eigenvalues are nearly the same as the negatives of the pole locations for a single nondepolarizing boundary (cf. Fig. 3). The large real eigenvalues are very nearly equal to the eigenvalues (4.11) for spin diffusion between two nondepolarizing boundaries with no field inhomogeneity.

of b; the criterion for validity is that the eigenfunction be well localized near one of the two boundaries and negligible near the other. Figure 7 shows the exact and asymptotic mappings of the circle $|b| = 28.669$ from the complex b plane into the complex γ plane. This circle goes through the second pair of real branch points $B = \pm 28.669$. The eigenfunction of (4.8) remains localized near one or the other boundary for a large range of $\arg b$, and the asymptotic mapping (4.20), shown by dashed lines, remains almost indistinguishable from the exact mapping, shown by solid lines, and obtained by numerical integration of (4.8). The asymptotic mapping fails in the neighborhood of branch points, where the eigenfunctions are affected by both boundaries and the exact mapping is very complicated.

Physically, the eigenfunctions shown in Fig. 6 represent the spatial distributions of transverse spin polarization that damp exponentially at the rate $\mathrm{Re}(\gamma)$ and precess at the rate $\mathrm{Im}(\gamma)$. The precession rate $\mathrm{Im}(\gamma)$ is proportional to the amount that the spiral is off-center, where the majority of the spins precess faster (or slower) than at the center of the interval.

B. Similarity to Mathieu functions

We note that the eigenfunctions and eigenvalues of (4.8) resemble the solutions $y = ce_0, ce_2, ce_4, \ldots$ of the Mathieu equation [15, 22, 23]

$$\frac{d^2y}{dx^2} + (a - 2q\cos 2x)y = 0. \tag{4.21}$$

These solutions have the period π and satisfy the boundary conditions $ce_n'(0) = ce_n'(\pi/2) = 0$, which are analogous to the boundary conditions (4.9). Sketched in Fig. 8 as a function of purely imaginary values of q are the eigenvalues $a_0, a_2, a_4, \ldots$, of $ce_0, ce_2, ce_4, \ldots$. Like the eigenvalues γ_n of Fig. 3, the eigenvalues of the Mathieu functions coalesce in successive pairs at branch points.

To understand the similarity, note that one can replace ζ in (4.8) by the periodic "potential" $V(\zeta + 4) = V(\zeta)$, which we define to be

$$V(\zeta) = \begin{cases} (\zeta + 2) & \text{if } -2 < \zeta < -1 \\ -\zeta & \text{if } -1 < \zeta < 1 \\ (\zeta - 2) & \text{if } 1 < \zeta \leq 2. \end{cases} \tag{4.22}$$

A solution ϕ of (4.8) with the boundary conditions (4.9) can be used to define a periodic function $y(\zeta + 4) = y(\zeta)$ on the real ζ axis by

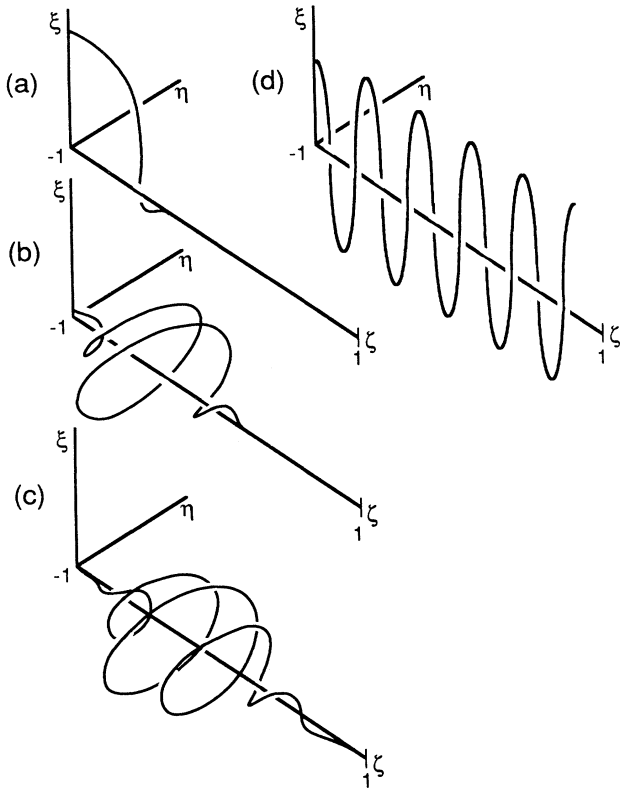

FIG. 6. The eigenfunctions ϕ_n of the time-independent Torrey equation (4.8). (a) $n = 0$, $b = 400$, $\gamma = 27.6 + 352i$; (b) $n = 6$, $b = 400$, $\gamma = 167 + 110i$; (c) $n = 12$, $b = 400$, $\gamma = 321$; (d) $n = 10$, $b = 2$, $\gamma = 247$. The eigenfunctions for the complex eigenvalues are very nearly the same as the eigenfunctions of (3.22) for diffusion to the right (or left) of a single nondepolarizing boundary. The eigenfunctions for sufficiently large real eigenvalues differ little from the delocalized sinusoids of (4.10).

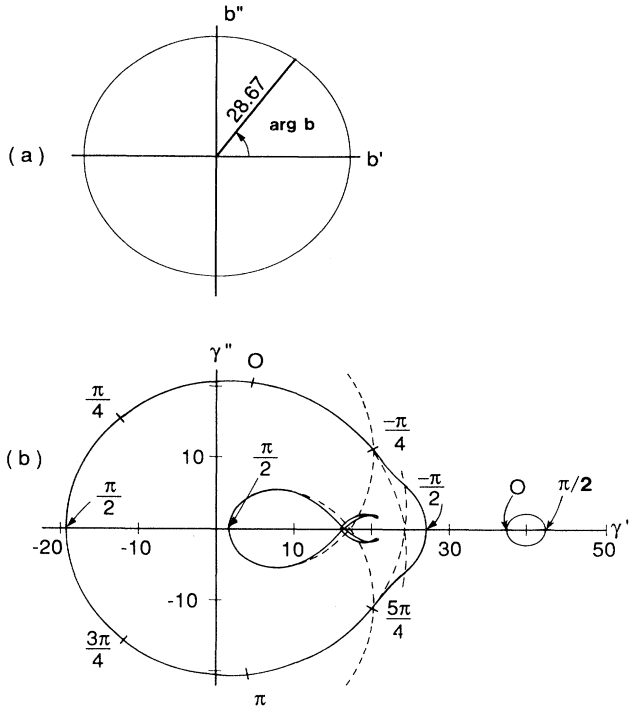

FIG. 7. Mapping of the circle $|b| = 28.67$ from (a) the complex b plane into (b) the complex γ plane. Several branches of the multivalued function $\gamma(b)$ are shown. For the higher sheets, one of which is shown near $\gamma = 40$, a single turn in the b plane produces two turns about a small circle in the γ plane. The first and second sheets of $\gamma(b)$ have coalesced. For these, one turn in the b plane maps to the single large loop in the γ plane. The third and fourth sheets just intersect at the branch point $\gamma = 16.55$, which corresponds to $b = \pm 28.67$.

$$y(\zeta) = \begin{cases} \phi(\zeta) & \text{if } -1 \le \zeta \le 1 \\ \phi(2-\zeta) & \text{if } 1 \le \zeta \le 3. \end{cases} \tag{4.23}$$

Then y is a solution of $y'' + \gamma y = ibVy$. The periodic functions y thus formed are Bloch functions of vanishing "crystal momentum" and even symmetry with respect to the points of the sawtooth potential (4.22). Both the Mathieu equation and the time-independent Torrey equation are Hill equations [24]. They depend on two complex parameters, a and q in the case of the Mathieu equation (4.21), and γ and b in (4.8). Meixner and Schäfke [25, 26] have shown that the existence of branch points, which they call *Ausnamewerte* or exceptional values, is a general property of eigenvalue equations that depend on two parameters. The solutions $ce_0, ce_2, ce_4, \ldots$, of the Mathieu equation for purely imaginary values of the parameter q describe the evolution of spin polarization transverse to the x axis in a thin cell with nondepolarizing walls at $x = 0$ and $x = \pi/2$ when the spins can simultaneously diffuse along the x direction and rotate around the x axis at a Larmor frequency proportional to $iq \cos 2x$. Presumably, a large class of periodic potentials similar to (4.22) will have eigenvalue spectra qualitatively similar to those of the Torrey equation and the Mathieu equation.

C. Eigenfunction expansions

One might surmise from (4.17) that the eigenfunctions ϕ_n form a complete set on the interval $[-1, 1]$, so the Green's function for (1.11) with two nondepolarizing boundaries should be

$$G(\zeta, \xi, \tau) = \sum_{n=0}^{\infty} N_n^2 \, \phi_n(\zeta)\phi_n(\xi) \exp(-\gamma_n \tau), \tag{4.24}$$

in analogy to (3.25). The normalization coefficients N_n are chosen such that

$$1 = N_n^2 \int_{-1}^{1} \phi_n^2(\zeta) d\zeta. \tag{4.25}$$

A proof that the expansion (4.24) is valid *except when*

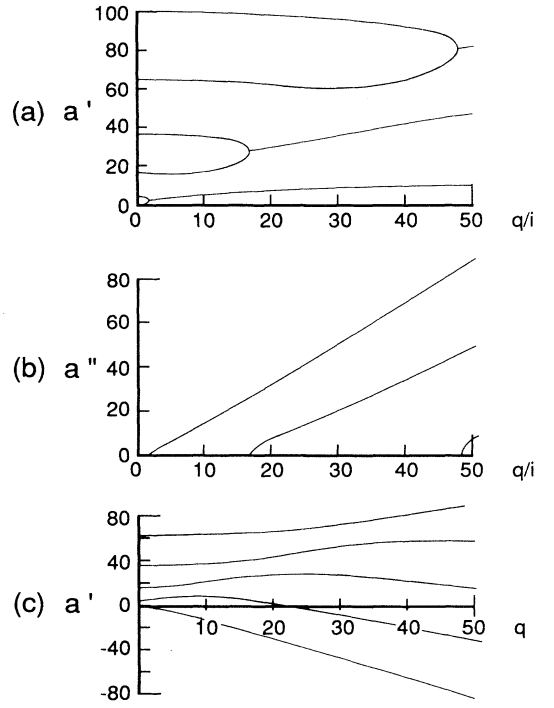

FIG. 8. (a) The real parts of the eigenvalues a of the Mathieu equation (4.21) for imaginary q. (b) The imaginary parts of the eigenvalues above. (c) The eigenvalues for real q; all eigenvalues are real. Note the qualitative similarity to the behavior of the eigenvalues of the Torrey equation, as shown in Fig. 3.

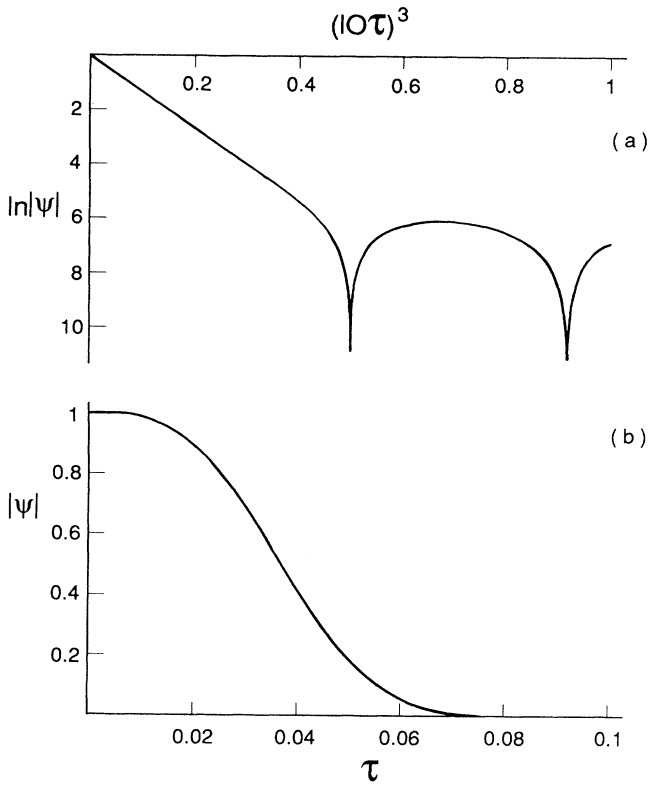

FIG. 9. Time dependence of the eigenfunction expansion of $\psi(\zeta,\tau)$ with the Green's function (4.24) at the center, $\zeta = 0$, of the spatial interval. The initial polarization was uniform, i.e., $\psi(\xi,0) = 1$. The expansion was truncated after the first 14 terms. The field inhomogeneity parameter was $b = 200$. (a) $\ln|\psi(0,\tau)|$ as a function of $(10\tau)^3$. The initial straight line is in excellent agreement with the predictions of Hahn's formula (2.34). The oscillations at late times are due to the eigenfunctions of the two left-most eigenvalues of Fig. 5. (b) $|\psi(0,\tau)|$ as a function of τ. On a linear scale, the oscillations at late time are hardly noticeable.

b is a branch point will be presented in Sec. V. However, a very convincing case for the validity can be made by examining the expansion with the numerically computed eigenfunctions and eigenvalues of (4.8). We found that the first 14 eigenfunctions at $b = 200$ represent the function $\psi(\zeta,0) = 1$ to better than 1%. In Fig. 9 we show the time dependence of $\psi(0,\tau) = \int_{-1}^{1} G(0,\xi,\tau)\psi(\xi,0)d\xi$, as given by the first 14 terms of the Green's function (4.24). As one can see from the logarithmic plot, the eigenfunction expansion decays exponentially with τ^3 at early times, in accordance with Hahn's formula (1.1). One can see from the linear plot that the oscillations at late times, which are due to the most slowly decaying eigenfunctions, are of no practical significance. Near the center of the interval and for large values of b, the series solution which follows from (4.24) is practically indistinguishable from the solution (2.34) for unbounded diffusion. There are increasingly noticeable differences from (2.34) as the position ζ moves closer to either boundary.

V. BRANCH POINTS

In this section we show that the eigenfunction expansion (4.24) is correct when b is not a branch point, and we discuss modifications that are necessary when b is a branch point. The resolvent $\tilde{G}(\zeta,\xi)$ for two nondepolarizing boundaries is a continuous function of ζ on the interval $-1 \le \zeta \le 1$ that satisfies the differential equation

$$(\lambda - H)\tilde{G}(\zeta,\xi) = \delta(\zeta - \xi), \tag{5.1}$$

where ξ is some source point on the interval and

$$H = \frac{\partial^2}{\partial\zeta^2} + ib\zeta. \tag{5.2}$$

The boundary conditions are

$$\frac{\partial\tilde{G}}{\partial\zeta} = 0 \quad \text{at} \quad \zeta = \pm 1. \tag{5.3}$$

Define two solutions u and v of the homogeneous equation

$$(\lambda - H)u = 0 \quad \text{and} \quad (\lambda - H)v = 0, \tag{5.4}$$

with the boundary conditions

$$u(-1)=1; \quad u'(-1)=0 \quad \text{and} \quad v(1)=1; \quad v'(1)=0, \tag{5.5}$$

where the prime denotes a partial derivative with respect to ζ. Here u and v are functions of the position ζ and of the complex parameters λ and b. For conciseness, we will write $u(\zeta)$ or simply u instead of $u(\lambda,b,\zeta)$ when the values of the arguments are clear from the context. Since the coefficients of the differential equations (5.4) have no singularities in the finite ζ plane, u and v are entire functions [27] of ζ. Also, $\partial u/\partial\lambda$ and $\partial u/\partial b$ are entire functions of ζ, defined by the inhomogeneous equations $(\lambda - H)\partial u/\partial\lambda = -u$ and $(\lambda - H)\partial u/\partial b = i\zeta u$, with $\partial u/\partial\lambda$, $\partial u/\partial b$, $\partial u'/\partial\lambda$ and $\partial u'/\partial b$ all equal to zero at $\zeta=-1$. Similar considerations hold for v. Thus, u and v are entire functions of λ and b. We use u and v to construct the function

$$\tilde{G}(\zeta,\xi)=\begin{cases} W^{-1}u(\zeta)v(\xi) & \text{if } \zeta<\xi \\ W^{-1}v(\zeta)u(\xi) & \text{if } \zeta>\xi, \end{cases} \tag{5.6}$$

where the Wronskian is

$$\begin{aligned} W=W(\lambda,b)&=v(\zeta)u'(\zeta)-v'(\zeta)u(\zeta)\\ &=u'(1)=-v'(-1). \end{aligned} \tag{5.7}$$

From (5.4) and (5.5) we see that the function (5.6) is a solution of (5.1) with the boundary conditions (5.3) and is therefore the resolvent. Since u, v, u', and v' are entire, the resolvent (5.6) is the ratio of entire functions.

Equation (5.4) implies that W is independent of ζ, so it can be conveniently evaluated at $\zeta=\pm1$ with the aid of (5.5) to give the last two equalities in (5.7). For any fixed value B of b, $\tilde{G}$ will have poles at those values λ_i of λ for which

$$W(\lambda_i,B)\equiv u'(\lambda_i,B,1)=0. \tag{5.8}$$

Let us consider values of λ and b near a pole,

$$\lambda=\lambda_i+\Delta\lambda \qquad \text{and} \qquad b=B+\Delta b. \tag{5.9}$$

We can expand u as a power series in $\Delta\lambda$ and Δb ,

$$\begin{aligned} u=u_{00}+\Delta\lambda\,u_{10}+\Delta b\,u_{01}+\frac{\Delta\lambda^2}{2}u_{20}+\Delta\lambda\Delta b\,u_{11}\\ +\frac{\Delta b^2}{2}u_{02}+\cdots, \end{aligned} \tag{5.10}$$

where

$$u_{pq}=\frac{\partial^{p+q}u}{\partial\lambda^p\partial b^q}(\lambda_i,B,\zeta). \tag{5.11}$$

Here

$$u_{00}=u(\lambda_i,B,\zeta), \tag{5.12}$$

so (5.5) and (5.8) imply that

$$u_{00}(-1)=1 \qquad \text{and} \qquad u'_{00}(\pm1)=0. \tag{5.13}$$

The partial derivatives of u satisfy the boundary conditions

$$u_{pq}(-1)=0 \quad \text{and} \quad u'_{pq}(-1)=0 \quad \text{for } pq\neq 00. \tag{5.14}$$

The analogous power series expansion of v is

$$\begin{aligned} v=v_{00}+\Delta\lambda\,v_{10}+\Delta b\,v_{01}+\frac{\Delta\lambda^2}{2}v_{20}+\Delta\lambda\Delta b\,v_{11}\\ +\frac{\Delta b^2}{2}v_{02}+\cdots, \end{aligned} \tag{5.15}$$

where

$$v_{00}=v(\lambda_i,B,\zeta) \tag{5.16}$$

with

$$v_{00}(1)=1 \quad \text{and} \quad v'_{00}(1)=0. \tag{5.17}$$

The boundary conditions for the partial derivatives of v are

$$v_{pq}(1)=0 \quad \text{and} \quad v'_{pq}(1)=0 \quad \text{for} \quad pq\neq 00. \tag{5.18}$$

Substituting the power series (5.10) into (5.4) and setting coefficients of $\Delta\lambda^p\Delta b^q$ equal to zero, we find that the expansion functions u_{pq} satisfy the differential equations

$$(\lambda_i-H)u_{00}=0, \tag{5.19a}$$

$$(\lambda_i-H)u_{pq}=-p\,u_{p-1,q}+q\,i\zeta\,u_{p,q-1} \quad \text{for} \quad pq\neq 00. \tag{5.19b}$$

In (5.19), the operator H is evaluated with $b=B$, and functions u_{pq} with negative values of p or q are understood to be identically zero. Substituting (5.15) into (5.4) shows that the v_{pq} satisfy the same differential equations (5.19) as the u_{pq}. The boundary conditions (5.14) and (5.18) together with the differential equations (5.19) fully determine the functions u_{pq} and v_{pq}.

We see that u_{00} is an eigenfunction of H with eigenvalue λ_i, satisfying the boundary conditions (5.13). It is identical to the eigenfunction ϕ discussed in connection with (4.8). The Laplace variable λ and the damping rate γ are related by $\lambda=-\gamma$.

Multiplying (5.19a) on the left by u_{p0}, multiplying (5.19b) with $q=0$ by u_{00}, and subtracting the equations which result gives the identity

$$u_{00}u''_{p0}-u''_{00}u_{p0}=p\,u_{p-1,0}u_{00}. \tag{5.20}$$

Integrating (5.20) we find

$$p\int_{-1}^{1}u_{00}u_{p-1,0}d\zeta=u_{00}(1)u'_{p0}(1). \tag{5.21}$$

In a similar manner we find

$$iq\int_{-1}^{1}\zeta u_{00}u_{0,q-1}d\zeta=-u_{00}(1)u'_{0q}(1). \tag{5.22}$$

We note that

$$u_{00}(1)\neq 0. \tag{5.23}$$

Indeed, since $u'_{00}(1)=0$ according to (5.13), if it were also true that $u_{00}(1)=0$, then (5.19a) would imply that $u_{00}\equiv 0$ for all values of ζ, in contradiction to (5.13).

We can think of the condition (5.8) as implicitly defining a function $\lambda_i=\lambda_i(B)$, which gives the location of the pole as a function of B. Using (5.10), (5.21), and (5.22) we find

$$\frac{d\lambda_i}{dB} = \frac{-u'_{01}(1)}{u'_{10}(1)} = \left(i\int_{-1}^{1}\zeta u_{00}^2\,d\zeta\right)\left(\int_{-1}^{1}u_{00}^2\,d\zeta\right)^{-1}. \tag{5.24}$$

Thus, there are singularities in the function $\lambda_i(B)$ at values of B when $u'_{10}(1) = 0$, or equivalently, when $\int_{-1}^{1}u_{00}^2\,d\zeta = 0$ and the function u_{00} is self-orthogonal. Although we will focus on the spectrum of pole locations λ_i for a fixed value B of b, there is a completely analogous viewpoint in which we consider the spectrum of pole locations b_i for a fixed value Λ of λ. There are singularities in the function $b_i(\Lambda)$ when $u'_{01}(1) = 0$, or equivalently, when $\int_{-1}^{1}\zeta u_{00}^2 d\zeta = 0$. Examples of both types of singularities are visible on Fig. 3, where the slope of one of the curves $\gamma(b)$ equals infinity or zero.

Substituting the series (5.10) and (5.15) into (5.7) we find, for $\Delta b = 0$,

$$W = (v_{00}u'_{00} - v'_{00}u_{00}) + \Delta\lambda(v_{00}u'_{10} + v_{10}u'_{00} - v'_{00}u_{10} - v'_{10}u_{00}) + \cdots \tag{5.25a}$$

$$= \Delta\lambda u'_{10}(1) + \frac{\Delta\lambda^2}{2!}u'_{20}(1) + \frac{\Delta\lambda^3}{3!}u'_{30}(1) + \cdots. \tag{5.25b}$$

The coefficient of each power of $\Delta\lambda$ in (5.25a) must be equal to the corresponding coefficient in (5.25b). Thus, the first term in parentheses is zero, and since this is the Wronskian of v_{00} and u_{00}, we conclude that

$$v_{00}(\zeta) = c\,u_{00}(\zeta) \qquad \text{where} \qquad c = \frac{1}{u_{00}(1)}. \tag{5.26}$$

The value of the coefficient c follows from the boundary conditions (5.17). Thus, when $\lambda = \lambda_i$ and $b = B$, the two solutions u and v of (5.4) are multiples of each other and it is impossible to find a function $\tilde{G}$ that is both continuous and has an appropriate discontinuity in the derivative at $\zeta = \xi$ to give the δ function in (5.1).

Similarly, equating the coefficients of $\Delta\lambda$ in (5.25) and using (5.26), we find

$$(cu'_{10} - v'_{10})u_{00} - (cu_{10} - v_{10})u'_{00} = u'_{10}(1), \tag{5.27}$$

which is valid for all values of ζ.

Inserting the series (5.10), (5.15), and (5.25) into (5.6), we find, for $\Delta b = 0$ and $\zeta < \xi$,

$$\tilde{G}(\zeta,\xi) = \frac{[u_{00}(\zeta) + \Delta\lambda\,u_{10}(\zeta) + \cdots][v_{00}(\xi) + \Delta\lambda\,v_{10}(\xi) + \cdots]}{\Delta\lambda\,u'_{10}(1) + \Delta\lambda^2\,u'_{20}(1)/2! + \Delta\lambda^3\,u'_{30}(1)/3! + \cdots}. \tag{5.28}$$

There is an analogous expression for $\zeta > \xi$. We see that the resolvent has a pole at $\lambda = \lambda_i$, and the order p of the pole is equal to the smallest value of p for which $u'_{po}(1) \neq 0$.

Consider a simple, first-order pole. Then

$$u'_{10}(1) \neq 0, \tag{5.29}$$

and (5.28) reduces to

$$\tilde{G}(\zeta,\xi) = \frac{u_{00}(\zeta)\,u_{00}(\xi)}{(\lambda - \lambda_i)u_{00}(1)u'_{10}(1)} + \cdots = \frac{N^2\phi(\zeta)\phi(\xi)}{\lambda - \lambda_i} + \cdots. \tag{5.30}$$

The singular term in (5.30) is the same for $\zeta > \xi$. The additional terms, indicated by the dots, remain finite as $\lambda \to \lambda_i$, but are different for $\zeta < \xi$ or $\zeta > \xi$. In accordance with the notation of (4.24) and (4.25) we have written

$$u_{00}(\zeta) = \phi(\zeta), \tag{5.31}$$

and

$$N^{-2} = \int_{-1}^{1}u_{00}^2 d\zeta = u_{00}(1)u'_{10}(1), \tag{5.32}$$

where the last equality follows from (5.21) with $p = 1$.

Now consider a double pole at $\lambda = \lambda_0$. Then

$$u'_{10}(1) = 0 \qquad \text{and} \qquad u'_{20}(1) \neq 0. \tag{5.33}$$

In view of (5.33), we conclude that the Wronskian (5.27) is zero, so for all values of ζ

$$(cu_{10} - v_{10}) = a\,u_{00} \quad \text{where} \quad a = \frac{u_{10}(1)}{[u_{00}(1)]^2}. \tag{5.34}$$

The value of the coefficient a can be determined by setting $\zeta = 1$ in (5.34) and using (5.18) and (5.26). Then (5.28) becomes

$$\tilde{G}(\zeta,\xi) = \frac{2}{u_{00}(1)u'_{20}(1)}\left\{\frac{u_{00}(\zeta)u_{00}(\xi)}{(\lambda - \lambda_0)^2} + \frac{1}{\lambda - \lambda_0}\left[u_{00}(\zeta)u_{10}(\xi) + u_{10}(\zeta)u_{00}(\xi) - \left(\frac{u_{10}(1)}{u_{00}(1)} + \frac{u'_{30}(1)}{3u'_{20}(1)}\right)u_{00}(\zeta)u_{00}(\xi)\right]\right\} + \cdots. \tag{5.35}$$

The singular terms in (5.35) are the same for $\zeta > \xi$. The additional terms, indicated by the dots, remain finite as $\lambda \to \lambda_0$, but are different for $\zeta < \xi$ or $\zeta > \xi$.

We have already shown that in the neighborhood of a simple pole, the rate of change of λ_i with b is finite and given by (5.24). For a second-order pole, (5.10) shows that it is possible to keep $u'(1) = 0$ if the lowest-order changes in λ and b are related by

$$\Delta b = -\frac{\Delta\lambda^2 u'_{20}(1)}{2u'_{01}(1)} \quad \text{or} \quad \Delta\lambda = \pm\left(\frac{-2u'_{01}(1)\Delta b}{u'_{20}(1)}\right)^{1/2} \tag{5.36}$$

The displacement Δb of the pole location in the b plane is second order in $\Delta\lambda$, the displacement of the pole location in the λ plane. One implication of this is that equal and opposite displacements of $\gamma = -\lambda$ from the branch point Γ correspond to the same value of b. An example is shown in Fig. 4.

Near a second-order branch point we can use (5.36) to write the eigenfunction (5.10) as

$$\phi = \Phi_0 + \Delta\lambda\,\Phi_1 + \cdots = \Phi_0 \pm \left(\frac{-2u'_{01}(1)\Delta b}{u'_{20}(1)}\right)^{1/2} \Phi_1 + \cdots, \tag{5.37}$$

where the eigenfunction at the branch point is

$$\Phi_0(\zeta) = u_{00}(\zeta), \tag{5.38}$$

and its rate of change with λ is

$$\Phi_1(\zeta) = u_{10}(\zeta). \tag{5.39}$$

From (5.32) and (5.33) we see that

$$M_{00} \equiv \int_{-1}^{1} \Phi_0^2\, d\zeta = 0. \tag{5.40}$$

With $p = 2$ in (5.21) we find

$$M_{01} \equiv \int_{-1}^{1} \Phi_0\Phi_1 d\zeta = \frac{1}{2}u_{00}(1)u'_{20}(1) \neq 0. \tag{5.41}$$

Multiplying both sides of (5.19b) by u_{10}, setting $p = 2$ and $q = 0$, and integrating gives

$$\begin{aligned} 2M_{11} \equiv 2\int_{-1}^{1} \Phi_1^2(\zeta)d\zeta &= -\int_{-1}^{1} u_{10}(\lambda_0 - H)u_{20}\, d\zeta \\ &= -\int_{-1}^{1} u_{20}(\lambda_0 - H)u_{10} d\zeta + u_{10}(1)u'_{20}(1), \end{aligned} \tag{5.42}$$

where the last equality is obtained by integrating by parts and using the boundary conditions (5.14) and (5.33). From (5.19) and (5.21) we find

$$\begin{aligned} \int_{-1}^{1} u_{20}(\lambda_0 - H)u_{10} d\zeta &= -\int_{-1}^{1} u_{20}u_{00} d\zeta \\ &= -\frac{1}{3}u_{00}(1)u'_{30}(1). \end{aligned} \tag{5.43}$$

With this (5.42) becomes

$$\begin{aligned} 2M_{11} &= u_{10}(1)u'_{20}(1) + \frac{1}{3}u_{00}(1)u'_{30}(1) \\ &= 2M_{01}\left(\frac{u_{10}(1)}{u_{00}(1)} + \frac{u'_{30}(1)}{3u'_{20}(1)}\right), \end{aligned} \tag{5.44}$$

and (5.35) becomes

$$\tilde{G}(\zeta,\xi) = \frac{1}{M_{01}}\left[\frac{\Phi_0(\zeta)\Phi_0(\xi)}{(\lambda-\lambda_0)^2} + \frac{1}{\lambda-\lambda_0}\left(\Phi_0(\zeta)\Phi_1(\xi) + \Phi_1(\zeta)\Phi_0(\xi) - \frac{M_{11}}{M_{01}}\Phi_0(\zeta)\Phi_0(\xi)\right)\right] + \cdots. \tag{5.45}$$

We can write the resolvent as the sum of all of its singular terms. If b is not one of the branch points, we simply sum the contributions (5.30) from the simple poles. Taking the inverse Laplace transform yields the familiar expansion (4.24), which is therefore complete if all of the singularities of $\tilde{G}(\zeta,\xi,\lambda)$ are simple poles in the λ plane.

The simple eigenvalue expansion (4.24) is not correct if b is one of the branch points, as one might expect since one of the eigenfunctions is lost. Equation (5.40) shows that Φ_0 is orthogonal to itself, so it is not possible to solve (4.25) for the corresponding normalization coefficient. If there are double poles, they must be excluded from the sum (4.24) and replaced by the inverse Laplace transform of (5.45),

$$\begin{aligned} \Delta G = \frac{e^{-\Gamma\tau}}{M_{01}}[\ &\Phi_0(\zeta)\Phi_1(\xi) + \Phi_1(\zeta)\Phi_0(\xi) \\ &+ (\tau - M_{11}/M_{01})\Phi_0(\zeta)\Phi_0(\xi)], \end{aligned} \tag{5.46}$$

where $\Gamma = -\lambda_i$. The solution at a branch point contains a term that evolves as $\tau e^{-\Gamma\tau}$, reminiscent of a critically damped oscillator.

The special form $ib\zeta$ of the "potential" for the Torrey equation allows us to find an explicit form for $\Phi_1 = u_{10}$, namely,

$$\Phi_1 = \frac{i\Phi'_0}{B} + r\Phi_0 + s\Theta_0. \tag{5.47}$$

The first term on the right-hand side of (5.47), when substituted into (5.19), yields the correct source term, $-u_{00}$, on the right-hand side of the equation. The coefficients r and s multiply independent solutions of the homogeneous equation, namely $\Phi_0 = u_{00}$, which we have already discussed, and a second solution Θ_0 which satisfies boundary conditions complementary to those of (5.13), which are

$$\Theta_0(-1) = 0 \quad \text{and} \quad \Theta'_0(-1) = 1. \tag{5.48}$$

The boundary conditions (5.13), (5.14), (5.33), and

(5.48) imply

$$r = 0 \quad \text{and} \quad s = 1 + \frac{i\Gamma}{B}, \tag{5.49}$$

so (5.47) becomes

$$\Phi_1 = \frac{i\Phi_0'}{B} + \left(1 + \frac{i\Gamma}{B}\right)\Theta_0. \tag{5.50}$$

One can carry through a similar analysis for higher-order branch points, but numerical studies show no evidence for their existence.

VI. REAL BRANCH POINTS

It is possible to find explicit expressions for the eigenvalues Γ and the expansion functions Φ_0 and Φ_1 at the real branch points B. For nonzero values of b we make the change of variables

$$w = \gamma/b^{2/3} + i\zeta b^{1/3} \quad \text{with} \quad \chi(w) = \phi(\zeta). \tag{6.1}$$

Then (4.8) becomes Airy's differential equation [16]

$$\chi'' = w\chi, \tag{6.2}$$

where the prime denotes differentiation with respect to w. The solutions of (4.8) with the boundary conditions (4.9) correspond to solutions of (6.2) with the boundary conditions

$$\chi' = 0 \quad \text{at} \quad w = w_\pm = \gamma/b^{2/3} \pm ib^{1/3}. \tag{6.3}$$

Let $p(w)$ and $q(w)$ be two independent solutions of (6.2) with the boundary conditions (6.3), and suppose that $p'(w_k) = 0$. We also assume that $p(w_k) \neq 0$ (or else we have the trivial solution $p(w) \equiv 0$). If $\delta\epsilon$ is an infinitesimal complex number, the derivative of the function

$$\chi(w) = p(w) + q(w)\,\delta\epsilon, \tag{6.4}$$

will have a zero at $w_k + \delta w_k$, where

$$\delta w_k = \frac{-q'(w_k)}{w_k p(w_k)}\delta\epsilon. \tag{6.5}$$

We have assumed that $w_k \neq 0$. For q to be independent of p we must have $q'(w_k) \neq 0$. Let two distinct zeros of p', $w_k = w_{\pm 1}$, define values of b and γ, according to (6.3). Then $b + \delta b$ and $\gamma + \delta\gamma$ correspond to $w_{\pm 1} + \delta w_{\pm 1}$, where

$$\delta b = \frac{3b^{2/3}}{2i}(\delta w_{+1} - \delta w_{-1}) \tag{6.6}$$

and

$$\delta\gamma = \frac{b^{2/3}}{2}(\delta w_{+1} + \delta w_{-1}) + \frac{2\gamma}{3b}\delta b. \tag{6.7}$$

Real branch points of the function $\gamma(b)$ occur where $db/d\gamma = 0$, or equivalently, where $\delta b = 0$.

Any solution of Airy's equation (6.2) can be written as a superposition of the two power series [15]

$$f(w) = 1 + \frac{1}{3!}w^3 + \frac{1\times 4}{6!}w^6 + \frac{1\times 4\times 7}{9!}w^9 + \cdots \tag{6.8}$$

and

$$g(w) = w + \frac{2}{4!}w^4 + \frac{2\times 5}{7!}w^7 + \frac{2\times 5\times 8}{10!}w^{10} + \cdots. \tag{6.9}$$

Here f and g are entire functions of w, which are related to the Bessel functions J_n of fractional order n by [15]

$$f(-z) = \frac{\sqrt{z}}{3^{1/3}\Gamma(2/3)}J_{-1/3}(\zeta) \tag{6.10}$$

and

$$g(-z) = \frac{\sqrt{z}}{3^{2/3}\Gamma(1/3)}J_{1/3}(\zeta), \tag{6.11}$$

where

$$\zeta = \frac{2}{3}z^{3/2}, \tag{6.12}$$

and Γ is the gamma function. Similarly,

$$f'(-z) = \frac{z}{3^{1/3}\Gamma(2/3)}J_{2/3}(\zeta) \tag{6.13}$$

and

$$g'(-z) = \frac{z}{3^{2/3}\Gamma(1/3)}J_{-2/3}(\zeta). \tag{6.14}$$

Denote a zero of $J_{-2/3}$ by j_p, that is,

$$J_{-2/3}(j_p) = 0. \tag{6.15}$$

Tables of the positive numbers j_p can be found in Ref. [28]. Setting $\zeta = j_p$ in (6.12) we find that each value of j_p gives three zeros of g', located at

$$w_{pn} = -\left(\frac{3j_p}{2}\right)^{2/3} e^{4\pi ni/3} \quad \text{for} \quad n = 0, \pm 1. \tag{6.16}$$

Suppose that

$$p = g \quad \text{and} \quad q = f. \tag{6.17}$$

From (6.8) and (6.9), the negative of the coefficient in (6.5) is

$$\frac{f'(w_{p,\pm 1})}{w_{p,\pm 1}g(w_{p,\pm 1})} = \frac{1}{2} + \frac{1}{120}\left(\frac{3j_p}{2}\right)^2 + \frac{1}{540}\left(\frac{3j_p}{2}\right)^4 + \cdots. \tag{6.18}$$

Therefore, (6.5) and (6.18) imply that $\delta w_{p,+1} = \delta w_{p,-1}$, and (6.6) implies that $\delta b = 0$. Thus, real branch points of $\gamma(b)$ occur when the eigenfunction of (6.2) is $\chi(w) = g(w)$.

From (6.3) and (6.16) we see that the branch point $b = B$ and the eigenvalue at the branch point $\gamma(B) = \Gamma$ must satisfy the equation

$$\left(\frac{3j_p}{2}\right)^{2/3} e^{\pm i\pi/3} = \Gamma/B^{2/3} \pm iB^{1/3}. \tag{6.19}$$

Solving (6.19) for B and Γ we find

$$\Gamma_p = \frac{B_p}{\sqrt{3}} = \frac{27}{32}j_p^2, \tag{6.20}$$

thus verifying (4.19). The first few values of B_p that follow from (4.21) were listed in Table II. The numerical calculations mentioned earlier suggest that all of the positive branch points are given by (6.20), and the symmetries of Table I imply that there are also branch points at $-B_p$.

From (5.13) we see that the properly normalized eigenfunction is

$$\Phi_0(\zeta) = u_{00}(\zeta) = \frac{g(w)}{g(w_-)}. \tag{6.21}$$

With the aid of (10.4.57) of Ref. [15] one can verify that (6.21) satisfies (5.40).

We can write the second solution of (5.4), defined by the boundary conditions (5.48), as

$$\Theta_0(\zeta) = r\,g(w) + s\,f(w). \tag{6.22}$$

The coefficients are found to be

$$s = \frac{1}{iB^{1/3}f'(w_-)} \quad \text{and} \quad r = \frac{-1}{iB^{1/3}f'(w_-)}\frac{f(w_-)}{g(w_-)}. \tag{6.23}$$

Substituting (6.21)–(6.23) into (5.50) gives

$$\Phi_1 = -B^{-2/3}\frac{g'(w)}{g(w_-)} + \frac{2e^{-i\pi/3}}{\sqrt{3}B^{1/3}}\frac{f(w_-)}{f'(w_-)}\left(\frac{f(w)}{f(w_-)} - \frac{g(w)}{g(w_-)}\right). \tag{6.24}$$

Other special values of the function $\gamma(b)$ can be found from tabulated zeros of χ' for solutions of the Airy equation (6.2), by substituting pairs of these zeros into (6.1), and solving for b and γ. Particularly useful are the functions f' and g' of (6.13) and (6.14), and the function Bi′, for which a number of the complex zeros have been tabulated by Olver [16, 29].

VII. SUMMARY

We have discussed the solutions of the Torrey equation for the relaxation of spins that are free to diffuse along one coordinate axis in the presence of an inhomogeneous magnetic field. In the limit of vanishing field inhomogeneity, the Torrey equation is identical to the well-known equation for heat diffusion in one dimension. The Torrey equation is also formally identical to the Schrödinger equation for a particle of imaginary mass accelerated by a constant force. The "Hamiltonian" is non-Hermitian, and there are interesting qualitative differences between the solutions of the Torrey equation and the more familiar solutions of the heat equation and the Schrödinger equation. We have discussed three different situations.

Unbounded diffusion. In Sec. II we derived the Green's functions and the resolvents for the Torrey equation in ordinary coordinate space and in momentum (spatial frequency) space for the case of unbounded diffusion. The Green's function (2.33) resembles a classical heat pole, and it leads naturally to Hahn's well-known result (1.1); the magnitude of initially uniform, transverse spin polarization decays exponentially with the cube of the time, the square of the field inhomogeneity, and the first power of the diffusion coefficient. In contrast to unbounded heat diffusion, where the resolvent kernel has a branch cut along the negative real axis in the plane of the Laplace variable, the resolvent (2.23) for the Torrey equation is an entire function of the Laplace variable and has an essential singularity at infinity.

One nondepolarizing boundary. In Sec. III we derived the resolvent for diffusion to the right or to the left of a nondepolarizing boundary. As shown by (3.14), the resolvent is the sum of the resolvent for free diffusion $\tilde{G}_0$, which is an entire function of the Laplace variable $\lambda = b^{2/3}s$, and a correction term $\tilde{G}_1$, which for real b has a line of simple poles in the negative half-plane, $\mathrm{Re}(s) < 0$, as shown in Fig. 2. The resolvent can be expressed as an eigenvalue expansion, which we write in abstract vector form as

$$\tilde{G} = \frac{1}{\lambda - H} = \sum_j \frac{|j\rangle\langle j|}{\lambda - \lambda_j}. \tag{7.1}$$

The projections onto the coordinate (ζ) axis are

$$\langle\zeta|j\rangle = \langle j|\zeta\rangle = N_j b^{1/6}\mathrm{Ai}(e^{-i\alpha}b^{1/3}(i\zeta - \lambda_j/b)). \tag{7.2}$$

The Airy function is appropriate for diffusion to the right of a boundary. The pole locations $\lambda_j = b^{2/3}s_j$ are given by (3.19), and the normalization coefficients N_j by (3.21). The phase angle is $\alpha = 2\pi/3$. The expansion (7.1) is reminiscent of similar expansions for the resolvent in quantum mechanics, but we note that the eigenfunction itself, not its complex conjugate, is the left factor in the expansion, and the eigenvalues λ_j have both real and imaginary parts.

Two nondepolarizing boundaries. Diffusion between two nondepolarizing boundaries is discussed in Secs. IV–VI. The negatives of the pole locations λ_j are the characteristic damping rates γ_j of the spin polarization, so we also use the variable $\gamma = -\lambda$. As shown by (4.2) and (4.3), the resolvent is the sum of the free-diffusion resolvent $\tilde{G}_0$ and a correction term $\tilde{G}_1$ with simple poles. In addition, $\tilde{G}_1$ has double poles at exceptional values of the field inhomogeneity b. We think of the eigenvalues γ of the time-independent Torrey equation (4.8) as different branches of the multivalued function $\gamma(b)$, where we allow b to be complex. Different sheets of $\gamma(b)$ connect at those values of b that produce double poles. Some of the branch points for real b are illustrated in Fig. 3. There are also branch points at complex values of b, one of which is illustrated in Fig. 4. We are not certain whether higher-order poles of $\tilde{G}$ and higher-order branch points of $\gamma(b)$ exist, but we have found no evidence for them in numerical studies of the Torrey equation. As illustrated in Fig. 5, the pole locations form a trigonal pattern for large real values of b. Some of the eigenfunctions are localized at one boundary, some at the other, and some are delocalized sinusoids.

The resolvent can be expressed as a sum of its singular parts, which we write as

$$\tilde{G} = \frac{1}{\lambda - H} = \sum_j \frac{P_j}{\lambda - \lambda_j} + \frac{Q}{\lambda - \lambda_0} + \frac{R}{(\lambda - \lambda_0)^2}. \quad (7.3)$$

The sum over j is the contribution from all of the simple poles of the resolvent. We assume that the field inhomogeneity b is equal to one of the exceptional values for which a double pole exists at $\lambda = \lambda_0$. The contribution from the double pole is described by the last two terms of (7.3), which therefore should be omitted if b is not one of the exceptional values. Numerical studies discussed above suggest there is never more than one double pole at an exceptional value of b. Should several double poles occur for the same value of b, one should sum over pairs of terms analogous to the last two terms of (7.3).

For a simple pole at λ_j

$$P_j = |j\rangle\langle j| \quad \text{with} \quad \langle\zeta|j\rangle = \langle j|\zeta\rangle = N_j\phi_j(\zeta). \quad (7.4)$$

The eigenfunction ϕ_j is determined by (4.8) with $\gamma = -\lambda_j$. The normalization coefficient N_j is given by (4.25).

For the double pole

$$Q = \frac{|0\rangle\langle 1| + |1\rangle\langle 0|}{\langle 0|1\rangle} - \frac{\langle 1|1\rangle}{\langle 0|1\rangle^2}|0\rangle\langle 0| \quad \text{and} \quad R = |0\rangle\langle 0|, \quad (7.5)$$

with

$$\langle\zeta|0\rangle = \langle 0|\zeta\rangle = \Phi_0(\zeta) \quad \text{and} \quad \langle\zeta|1\rangle = \langle 1|\zeta\rangle = \Phi_1(\zeta). \quad (7.6)$$

Here Φ_0 is the eigenfunction at the double pole λ_0 of the resolvent, as defined by (5.38), (5.19a), and (5.13), and Φ_1 is not an eigenfunction but is the rate of change of Φ_0 with λ, as defined by (5.39), (5.19b), and (5.14).

Since the eigenfunctions ϕ_j at the simple poles can be normalized, as shown by (5.32), the projectors P_j are mutually orthonormal and are orthogonal to Q and R,

$$P_jP_k = \delta_{jk} \quad \text{and} \quad P_jQ = QP_j = P_jR = RP_j = 0. \quad (7.7)$$

In view of the self-orthogonality (5.40) of the branch-point eigenfunction, namely, $\langle 0|0\rangle = 0$, we find

$$R^2 = 0; \qquad QR = RQ = R; \qquad Q^2 = Q. \quad (7.8)$$

If we expand (7.3) in powers of $1/\lambda$ and equate coefficients of $1/\lambda$ and $(1/\lambda)^2$ we find

$$1 = \sum_j P_j + Q \quad (7.9)$$

and

$$H = \sum_j \lambda_j P_j + \lambda_0 Q + R. \quad (7.10)$$

Equation (7.9) expresses the completeness of the eigenfunctions, when augmented by Φ_1, which is not an eigenfunction. The expansion (7.10) of the Hamiltonian is reminiscent of similar expansions in elementary quantum mechanics, but the additional term R and the form (7.5) of Q are unusual, since branch points do not occur for Hermitian operators in one dimension. The locations of the real branch points are given explicitly by (6.20).

The existence of branch points is a general property of equations similar to the Torrey equation for two nondepolarizing boundaries [25,26]. The dependence of the eigenvalues of the Mathieu equation on the depth of the sinusoidal potential is shown in Fig. 8. These plots could easily be mistaken for those of the Torrey equation, Fig. 3.

Because of the branch points which occur in the multivalued function $\gamma(b)$, the radii of convergence of the perturbation expansions used to express the spin-relaxation rate γ as power series in b cannot be larger than the first branch point of the sheet of interest. In the case of the simple Torrey equation, the power series expansion of γ_0, the leading term of which is given by (4.13), fails when $b = 2.2581$, the first exceptional value, as given in Table II.

For large values of the field inhomogeneity b, or equivalently, for large displacements l of the boundaries from the origin, one can very nearly ignore the boundaries. This is confirmed by numerical studies of the Torrey equation, like those of Fig. 9, and by the form of the corrections $\tilde{G}_1$, given by (3.15) and (4.3), to the free-diffusion resolvent $\tilde{G}_0$ of (2.23). From the known asymptotic behavior of Airy functions, it is straightforward to show that $G_1 \to 0$ as $|l| \to \infty$.

ACKNOWLEDGMENTS

The authors are grateful for helpful discussions with many colleagues, including M. Aizenmann, C. Callan, G. Cates, E. Lieb, F. W. Olver, O. Rothaus, and S. Treiman. This work was supported by the U. S. Air Force Office of Scientific Research, under Grant No. AFOSR-88-0165.

[1] E. L. Hahn, Phys. Rev. **80**, 580 (1950).
[2] H. Y. Carr and E. M. Purcell, Phys. Rev. **94**, 630 (1954).
[3] H. C. Torrey, Phys. Rev. **104**, 563 (1956).
[4] G. D. Cates, S. R. Schaefer, and W. Happer, Phys. Rev. A **37**, 2877 (1988).
[5] Douglas D. McGregor, Phys. Rev. A **41**, 2631 (1990).
[6] G. D. Cates, D. J. White, Ting-Ray Chien, S. R. Schaefer, and W. Happer, Phys. Rev. A **38**, 5092 (1988).
[7] K. C. Hasson, G. D. Cates, K. Lerman, P. Bogorad, and W. Happer, Phys. Rev. A **41**, 3672 (1990).
[8] Z. Wu, S. R. Schaefer, G. D. Cates, and W. Happer, Phys. Rev. A **37**, 1161 (1988).
[9] U. Fano, Rev. Mod. Phys. **29**, 74 (1957).
[10] R. L. Gamblin and T. R. Carver, Phys. Rev. A **138**, 946 (1965).
[11] L. D. Schearer and G. K. Walters, Phys. Rev. A **139**, 1398 (1965).
[12] R. Barbé, M. Leduc, and F. Laloë, J. Phys. (Paris) **35**,

699 (1974); **35**, 935 (1974).
[13] V. Lefèvre-Seguin, P. J. Nacher, and F. Laloë, J. Phys. (Paris) **43**, 737 (1982).
[14] C. P. Slichter, *Principles of Magnetic Resonance* (Harper and Row, New York, 1963).
[15] M. Abramowitz and I. A. Stegun, *Handbook of Mathematical Functions* (Dover, New York, 1965).
[16] F. W. Olver, *Asymptotics and Special Functions* (Academic, New York, 1974).
[17] A. Sommerfeld, *Partial Differential Equations* (Academic, New York, 1949).
[18] D. J. Schneider and J. H. Freed, Adv. Chem. Phys. **73**, 387 (1989).
[19] B. Robertson, Phys. Rev. **151**, 273 (1966).
[20] J. H. Freed, Ann. Phys. Fr. **10**, 901 (1985); B. R. Johnson and J. Freed, Phys. Rev. Lett. **52**, 1508 (1984); N. Bigelow, J. Freed, and D. Lee, *ibid.* **63**, 1609 (1989).
[21] W. H. Press, B.P. Flannery, S. A. Teukolsky, and W. T. Vetterling, *Numerical Recipes, The Art of Scientific Computing* (Cambridge University, Cambridge, 1986).
[22] E. Jahnke and F. Emde, *Tables of Functions with Formulae and Curves* (Dover, New York, 1945).
[23] G. Blanch and D. S. Clemm, *Mathieu's Equation for Complex Parameters* (U.S. GPO, Washington, DC, 1969).
[24] W. Magnus and S. Winkler, *Hill's Equation* (Dover, New York, 1979).
[25] J. Meixner and F. W. Schäfke, *Mathieusche Functionen und Sphäroidfunctionen* (Springer, Berlin, 1954).
[26] J. Meixner, F.W. Schäfke, and G. Wolf, *Mathieu Functions and Spheroidal Functions and Their Mathematical Foundations* (Springer, Berlin, 1980).
[27] E. T. Whittaker and G. N. Watson, *A Course of Modern Analysis* (Cambridge, New York, 1963).
[28] U. S. National Bureau of Standards, *Tables of Bessel Functions of Fractional Order* (Columbia University Press, New York, 1948).
[29] F. W. Olver, Philos. Trans. R. Soc. London Sec. A **247**, 328 (1954).